Journal of Medicinal Chemistry

Article

pubs.acs.org/jmc

Synthesis and Biological Evaluation of Novel Olean-28,13β-lactams as Potential Antiprostate Cancer Agents

Yong Ai,[†,‡,∥] Yang Hu,[†,∥] Fenghua Kang,[†,‡] Yisheng Lai,[†,‡] Yanju Jia,[†] Zhangjian Huang,*[,†,‡] Sixun Peng,[†,‡] Hui Ji,*[,†] Jide Tian,[§] and Yihua Zhang*[,†,‡]

[†]State Key Laboratory of Natural Medicines, China Pharmaceutical University, Nanjing 210009, P. R. China

[‡]Jiangsu Key Laboratory of Drug Discovery for Metabolic Diseases, China Pharmaceutical University, Nanjing 210009, P. R. China

[§]Department of Molecular and Medical Pharmacology, University of California, Los Angeles, California 90095, United States

Supporting Information

ABSTRACT: γ-Lactam is an important structural motif in a large number of biologically active natural products and synthetic small pharmaceutical molecules. However, there is currently no effective approach to construct γ-lactam ring directly from natural rigid polycyclic amides. Herein, we report a facile methodology for synthesis of a new group of olean-28,13β-lactams (**10a−j**) from their corresponding amides, promoted by an easily available reagent 2,3-dichloro-5,6-dicyanobenzoquinone (DDQ), through an intramolecular dehydrogenative C−N coupling reaction via a radical ion mechanism. Biological evaluation indicated that the most active lactam **10h** displayed potent antiproliferative activity against human cancer cells but 13.84- to 16.92-fold less inhibitory activity on noncancer cells in vitro. In addition, **10h** significantly inhibited the growth of implanted prostate cancer in vivo. Furthermore, **10h** induced cell cycle arrest and apoptosis and down-regulated the AKT/mTOR signaling in DU-145 cells. Finally, **10h** was more stable in rat plasma and human liver microsomes than CDDO-Me and had little hERG channel inhibitory activity. Collectively, **10h** may be a potential antiprostate cancer agent for further investigation.

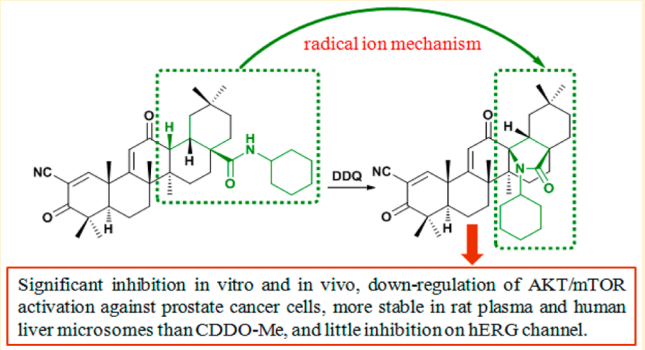

INTRODUCTION

Oleanolic acid (OA) is a well-known natural triterpenoid and has multiple pharmacological activities.[1] To improve its potency, a large number of synthetic OA derivatives (SOADs) have been prepared, including 2-cyano-3,12-dioxooleana-1,9(11)-dien-28-oic acid (CDDO), its ester (CDDO-Me) and amide (CDDO-Im) (Figure 1), and others.[2,3] Compared with OA, these SOADs

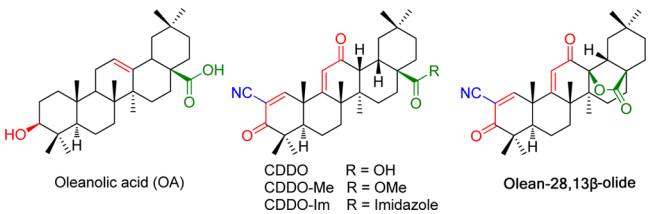

Figure 1. Chemical structures of OA and SOADs.

have much stronger anti-inflammatory and antitumor activities by activating cytoprotective pathways[4] and inducing cancer cell apoptosis.[5] CDDO-Me has been tested in clinical trials for treatment of advanced solid tumors and lymphoid malignancies.[6] We have also synthesized SOADs for the intervention of cancers[7−10] and discovered the olean-28,13β-olide, a γ-lactone compound, with potent in vitro and in vivo anticancer activity comparable to CDDO-Me.[11,12]

γ-Lactam, like γ-lactone, is an important structural motif in a large number of biologically active natural products[13−20] and synthetic small pharmaceutical molecules for the treatment of cancer,[13,19−21] fungal infection,[20] chemotherapy-induced nausea and vomiting,[22] Alzheimer's disease,[23] and human immunodeficient virus (HIV) infection.[24] For example, the γ-lactam moiety in the inhibitors of histone deacetylase (HDAC) can fit into the narrow hydrophobic pocket of HDAC active site better than the larger δ-lactam moiety and has more potent enzymatic inhibitory and antiproliferative activities.[22] However, there currently is no effective approach to construct γ-lactam ring directly from natural rigid polycyclic amides. In this context, we hypothesized that synthesis of novel olean-28,13β-lactams from their corresponding amides could generate a new class of SOADs with potent anticancer activity. To address the hypothesis, lactam compounds **10a−j** were designed and synthesized and their antitumor activities were evaluated in vitro and in vivo.

Received: December 24, 2014

DOI: 10.1021/jm5020023
J. Med. Chem. XXXX, XXX, XXX−XXX

Scheme 1. Synthetic Route of Olean-28,13β-lactams 10a−j[a]

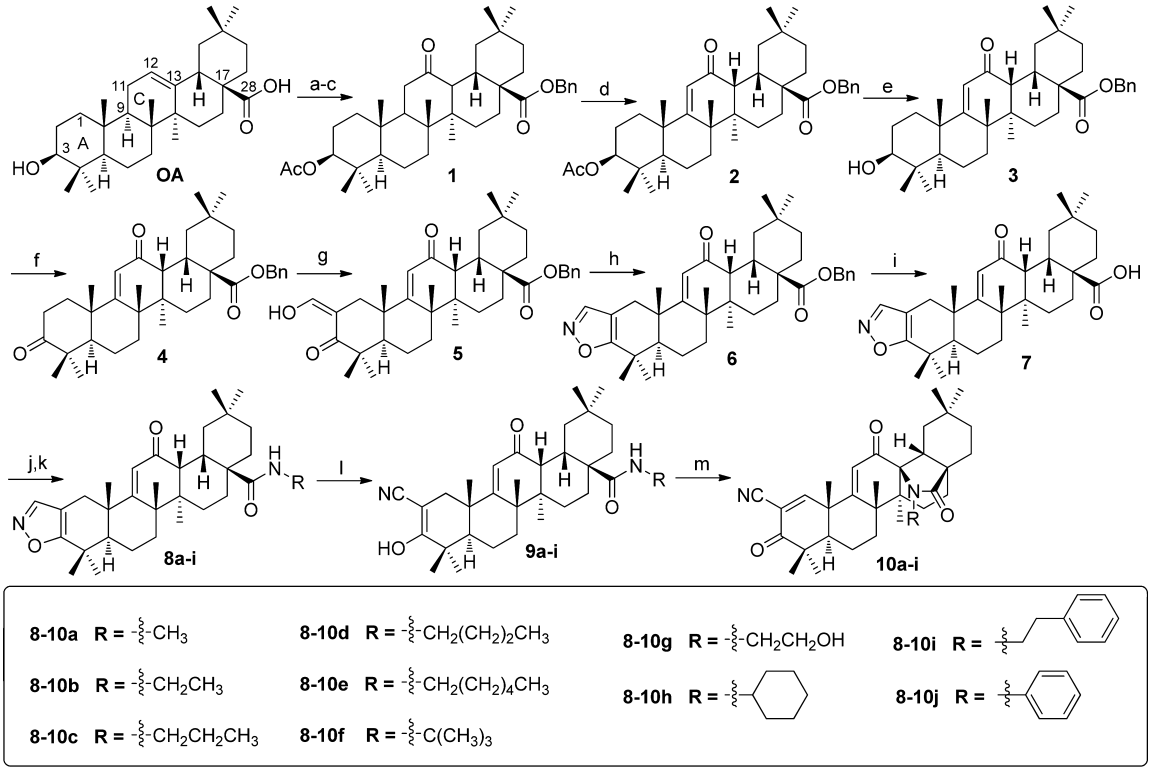

[a]Reagents and conditions: (a) BnCl, K_2CO_3, DMF, 50 °C, 4 h; (b) Ac_2O, pyridine, rt, 4 h; (c) 30% H_2O_2, HCO_2H, CH_2Cl_2, rt, 24 h; (d) Br_2, HBr, AcOH, 50 °C, 24 h; (e) KOH, MeOH, reflux, 45 min; (f) Jones reagent, acetone, 0 °C → rt, 20 min; (g) HCO_2Et, NaOMe, anhydrous CH_2Cl_2, rt, 2 h; (h) $NH_2OH{\cdot}HCl$, EtOH, reflux, 1 h; (i) H_2, Pd/C, THF, atmospheric pressure, rt, 0.5 h; (j) $(COCl)_2$, anhydrous CH_2Cl_2, 0 °C → rt, 12 h; (k) primary amine, TEA, anhydrous CH_2Cl_2, 0 °C → rt, 12 h; (l) NaOMe, MeOH, Et_2O, 0 °C → rt, 1 h; (m) DDQ, anhydrous methylbenzene, 80−110 °C, 8−24 h.

RESULTS AND DISCUSSION

Chemistry. The target compounds **10a−j** were synthesized as depicted in Scheme 1. A bromination reaction of ketone **1**, which was prepared starting from OA as described previously,[11] followed by dehydrobromination led to enone **2**. The removal of the acetyl at 3-acyloxy group of **2** by KOH in methanol freed the 3-hydroxy group, and the resulting compound **3** underwent a Jones oxidation giving the diketone **4**. Formylation at C-2 was performed in the presence of ethyl formate and sodium methoxide in dichloromethane furnishing an enolate **5**, which was cyclized into isoxazole **6** by treatment with hydroxylamine hydrochloride in aqueous ethanol. Debenzylation at C-28 of **6** was carried out in tetrahydrofuran using 10% Pd/C as the catalyst to give free acid **7**, which was converted to its acyl chloride using oxalyl chloride, and without further purification the acyl chloride was treated with corresponding primary amines to yield amides **8a−j**. The isoxazole ring in **8a−j** was opened in the presence of sodium methoxide, affording 2-cyanoenolates **9a−j**. Finally, the 1,2-double bond and 28,13β-lactam functionalities were generated in a one-pot procedure via a dehydrogenation reaction mediated by 2,3-dichloro-5,6-dicyano-1,4-benzoquinone (DDQ) in toluene to provide the target lactams **10a−i**.

It is notable that the yields of the last step reaction were affected by the steric hindrance and/or electronic effect of the substituent (R) at the nitrogen atom. As shown in Table 1, entries 1−5, when R was occupied by bulkier group, the yields tended to decrease. On the other hand, compound **10i** containing an electron-withdrawing phenyl group at 2-position of ethyl was much more difficult to be obtained than compound **10b** with only an electron-donating ethyl group (110 °C, 24 h, 45% vs 80 °C, 6 h, 69%, respectively). Similarly, when a cyclohexyl group (**10h**) was replaced by a phenyl group (**10j**), no product was obtained. These results suggest that a smaller and/or electron-donating substituent may be beneficial for dehydrogenation to build a 28,13β-lactam ring.

The mechanism underlying the formation of olean-28,13β-lactams (**10a−i**) promoted by DDQ may be similar to that of the generation of olean-28,13β-olides we proposed previously.[11] The 2-cyanoenone functionality is constructed from

Table 1. Reaction Conditions and Yields of Olean-28,13β-lactams (10a−j)[a]

entry	product	R	reaction conditions	isolated yield, %[b]
1	**10a**	-CH_3	80 °C, 4 h	75
2	**10b**	-CH_2CH_3	80 °C, 6 h	69
3	**10c**	-$CH_2CH_2CH_3$	80 °C, 6 h	65
4	**10d**	-$CH_2(CH_2)_2CH_3$	80 °C, 8 h	60
5	**10e**	-$CH_2(CH_2)_4CH_3$	90 °C, 12 h	58
6	**10f**	-$C(CH_3)_3$	90 °C, 5 h	60
7	**10g**	-CH_2CH_2OH	90 °C, 10 h	55
8	**10h**	-cyclohexyl	90 °C, 12 h	68
9	**10i**	-CH_2CH_2Ph	110 °C, 24 h	45
10	**10j**	-Ph	reflux, >24 h	0

[a]All reactions were performed with 2 equiv of DDQ in anhydrous toluene. [b]Yield of the isolated product based on the reacted substrate.

DOI: 10.1021/jm5020023
J. Med. Chem. XXXX, XXX, XXX−XXX

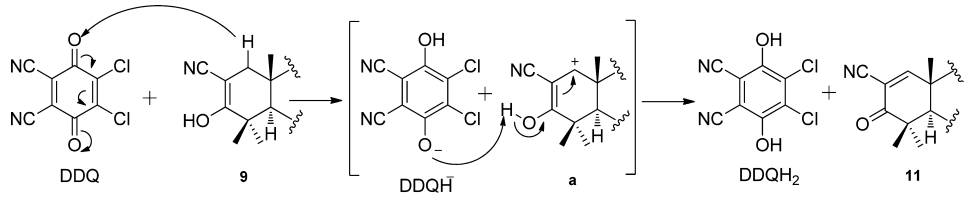

Figure 2. A proposed ionic mechanism for the dehydrogenation of ring A of compound **9**.

Table 2. Reactions of 9h with Various Amounts of DDQ at Different Times[a]

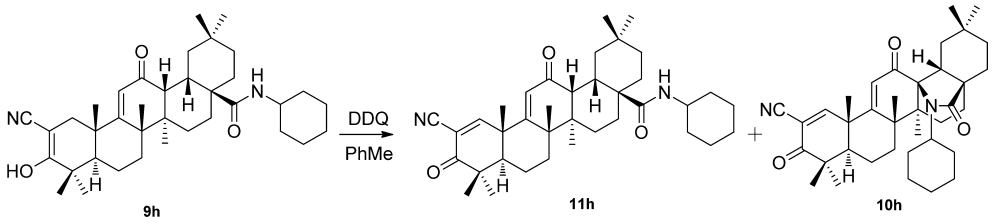

entry	DDQ (equiv)	time (h)	yield of **11h** (%)[b]	yield of **10h** (%)[b]
1	0.5	0.5	43	0
2	0.5	12	45	0
3	1	0.5	89	0
4	1.5	0.5	80	10
5	1.5	12	65	21
6	2	12	<10	68

[a]All reactions were performed with DDQ at 90 °C in anhydrous toluene. [b]Yield of the isolated products.

dehydrogenation on ring A of compound **9** via an ionic mechanism, and the lactam ring is built from the amide moiety in the same compound via a radical ion mechanism.

The ionic mechanism is shown in Figure 2. DDQ first abstracts a hydrogen anion from enolate **9** leading to an oxygen anion of DDQ ($DDQH^-$) and a carbon cation **a**. Subsequently, the $DDQH^-$ captures a proton from the intermediate **a**, generating a 2-cyanoenone product **11** (as shown in Table 2) and $DDQH_2$.

To clarify this point, the **9h** was reacted with various amounts of DDQ for different time periods. The reaction of **9h** with ≤1 equiv of DDQ for half an hour led to generation of only compound **11h** (Table 2, entries 1−3). However, the reaction of **9h** with >1 equiv of DDQ, particularly with 2 equiv of DDQ, for longer heating in toluene generated the lactam **10h** in a dose- and time-dependent manner (Table 2, entries 4−6). These results indicated that the DDQ-mediated dehydrogenation of ring A occurred prior to the construction of the lactam ring and that the subsequent transformation of **11** into **10** proceeded via a distinct mechanism.

On the basis of the above results, we speculate that the lactam **10h** may be produced from the amide **11h** by DDQ promotion. Indeed, when we heated **11h** with 1 equiv of DDQ for several hours, **10h** was obtained (Scheme 2). Similarly, the lactams **13h** and **15** could also be produced from the corresponding amides **8h** and **14** under the same conditions, thus confirming our speculation.

The construction of the lactam ring may proceed via a radical ion mechanism as depicted in Figure 3. DDQ first traps an electon from the electron-rich enone on the ring C of **11** to produce a radical cation **b** and a radical anion $DDQ^{\bullet -}$. Subsequent hemolytic cleavage of the C−H bond at the C13 position results in an enol radical cation **c**. Then the nitrogen atom with a pair of electrons on the C28-carboxylic amide of **c** acts as a nucleophile to attack C13, followed by deprotonation

Scheme 2. Olean-28,13β-lactams (10h, 13h, and 15) Produced from the Corresponding Amides (11h, 8h, and 14) Promoted by DDQ

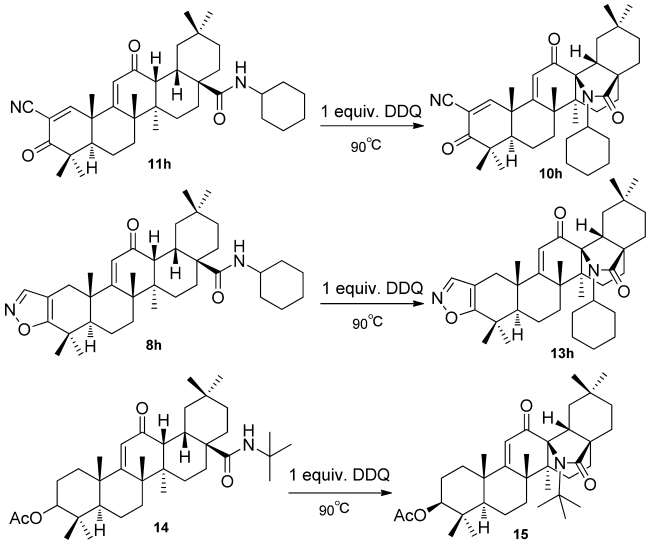

to form a lactam radical **d** and $DDQH^{\bullet}$. The intermediate **d** is subsequently oxidized by $DDQH^{\bullet}$ to generate cation **e** and $DDQH^-$. Finally, **e** is deprotonated by $DDQH^{\bullet}$ to provide **10** and $DDQH_2$. According to the mechanism mentioned above, the substituent R on the nitrogen of amides **9a−j** in Scheme 1 may be a rate-limiting factor, and a smaller and/or electron-donating substituent is beneficial to build a 28,13β-lactam ring.

To verify the proposed radical ion mechanism in the formation of lactam via an enol as a transient intermediate **c** (Figure 3), compound **8h**, which could be converted to the corresponding lactam **13h** as mentioned above, was treated with acetyl chloride in the presence of DDQ. Fortunately, the

DOI: 10.1021/jm5020023
J. Med. Chem. XXXX, XXX, XXX−XXX

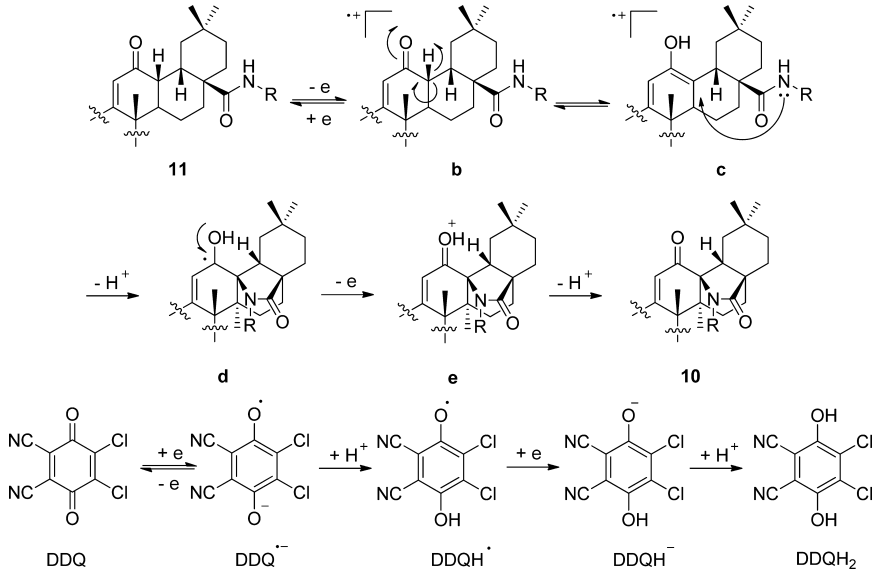

Figure 3. A proposed radical ion mechanism for the DDQ-mediated formation of γ-lactam ring of **10a–j**.

Table 3. Evidence for an Enol as a Transient Intermediate in the DDQ-Promoted Formation of Olean-28,13β-lactam[a]

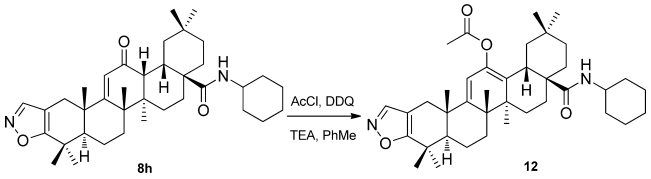

entry	8h (equiv)	AcCl (equiv)	DDQ (equiv)	temp (°C)	isolated yield of 12, %[b]
1	1.0	10	0	90	0
2	1.0	0	1.1	90	0
3	1.0	10	1.1	25	0
4	1.0	1	1.1	90	trace
5	1.0	10	1.1	90	21

[a]All reactions were performed with 2 equiv of TEA and run for 24 h in anhydrous toluene. [b]Yield of the isolated product based on the reacted substrate.

O-acetylated enolate **12h** was successfully isolated and identified in Table 3, suggesting that long-term heating- and DDQ-promoted enolization of the ketone on ring C of **11** may be involved in the generation of the lactam ring of **10**, which is in agreement with the radical ion mechanism.

Biological Activity. *Assessment of in Vitro Antiproliferative Activity.* Compounds **10a–i** and **11h** were preliminarily screened for their inhibitory activitiy against human prostate carcinoma DU-145 cell proliferation by CCK-8 assay using CDDO-Me as a positive control. As shown in Figure 4, most of compounds at 2 μM displayed varying inhibitory activities. **10h** exhibited the most potent inhibitory activity (75%), which was statistically higher than that of its precursor amide **11h** (53%) and positive control CDDO-Me (63%). Since this study on small numbers of compounds may have no conclusive data for structure–activity relationship (SAR), we are interested in further expanding the compound library to analyze the SAR.

The active compounds **10f** and **10h** were further assayed for their antiproliferative activity against four human cancer cell lines, DU-145 (human prostate cancer cells), H460 (human non-small-cell lung cancer cells), Bxpc-3 (human pancreatic

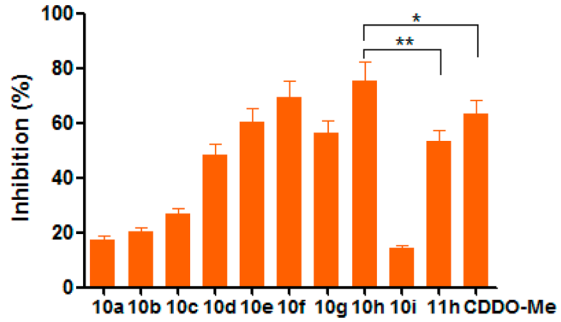

Figure 4. Inhibition of DU-145 cell proliferation. DU-145 cells were treated with, or without, the indicated compounds at 2 μM for 72 h, and the cell proliferation was measured. The inhibition (%) of each compound was determined. Data are presented as the mean (%) ± SD of each compound from three independent experiments: (*) $P < 0.05$ vs CDDO-Me; (**) $P < 0.01$ vs **11h**.

carcinoma cells), and BEL-7404 (human hepatocellular carcinoma cells), and human nontumor cell line WPMY-1 (human prostatic stromal myofibroblast cells). The IC_{50} values of **10h** were from 0.33 to 0.46 μM against all four types of cancer cells, comparable to CDDO-Me and stronger than CDDO-Im and **10f**. Significantly, **10h** had 13.84- to 16.92-fold less inhibitory activity against nontumor WPMY-1 (IC_{50} = 6.09 μM) than against all cancer cells tested. Hence, **10h** preferably inhibits the proliferation of cancer cells, superior to CDDO-Me and CDDO-Im (Table 4).

In Vivo Anticancer Activity of ***10h****.* To evaluate the safety of **10h**, adult ICR mice were randomly treated by oral gavage with a single dose of **10h** at 800, 640, 512, 409.6, and 327.8 mg/kg based on our preliminary study, and the survival of the mice was monitored up to 14 days after treatment (Table 5). While treatment with a large dose (800 mg/kg) of **10h** killed all mice, treatment with 327.8 mg/kg did not cause any death or abnormality in eating, drinking, body weight, or activity throughout the observation period. As a result, the LD_{50} value of **10h** was 540.7 mg/kg for this strain of mice.

To evaluate the in vivo anticancer activity of **10h**, male BALB/c nude mice were inoculated subcutaneously with human prostate carcinoma DU-145 cells. After the establishment

DOI: 10.1021/jm5020023
J. Med. Chem. XXXX, XXX, XXX–XXX

Table 4. Antiproliferative Activity of Compounds

	IC_{50} (μM)[a]				
compd	DU-145	H460	Bxpc-3	BEL-7404	WPMY-1
10h	0.39 ± 0.03[b]	0.38 ± 0.03	0.33 ± 0.03	0.46 ± 0.03[b]	6.09 ± 0.53[b]
10f	0.96 ± 0.08	0.43 ± 0.04	0.66 ± 0.06	1.14 ± 0.10	9.60 ± 0.81[b]
CDDO-Im	0.69 ± 0.05	0.42 ± 0.04	1.50 ± 0.12	0.99 ± 0.07	2.09 ± 0.14
CDDO-Me	0.53 ± 0.03	0.40 ± 0.02	0.24 ± 0.02	0.81 ± 0.07	1.86 ± 0.11

[a]Data are expressed as mean IC_{50} ± SD (μM) of each compound from three independent experiments. IC_{50} is the drug concentration inhibiting 50% of the cell proliferation. [b]$P < 0.01$ vs CDDO-Me.

Table 5. Acute Toxicity of 10h in Mice

		mouse mortality						
dose (mg/kg)	no. of mice	1 h	4 h	3 d	4−14 d	total mortality	survival (%) on day 14	LD_{50}[a] (mg/kg)
800	8	1	2	5	0	8	0	
640	8	0	0	6	0	6	25	
512	8	0	0	3	0	3	63	540.7
409.6	8	0	0	1	0	1	88	
327.8	8	0	0	0	0	0	100	

[a]The 95% confidence limits: 475.7−614.66 mg/kg.

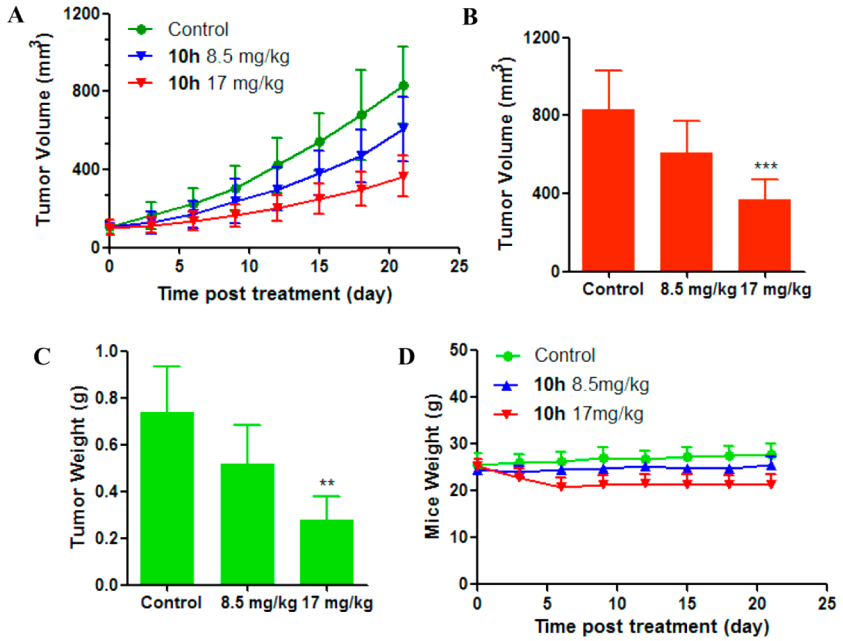

Figure 5. Inhibitory effects of **10h** on the growth of implanted prostatic tumors in mice. Male nude mice were inoculated with DU-145 cells, and after establishment of solid tumors, the mice were randomly treated with the indicated doses of **10h** or vehicle daily, followed by monitoring of the growth of tumors in mice: (A) dynamic growth of implanted tumors in mice; (B) tumor volumes in mice measured on the last day of the experiment; (C) tumor weights in mice; (D) body weight changes in mice. Data are expressed as the mean ± SD from each group of mice ($n = 5$ per group): (**) $P < 0.01$, (***) $P < 0.001$ vs the vehicle-treated control.

of solid tumor, the mice were randomly treated by gavage with **10h** and vehicle daily for 21 consecutive days, respectively. While treatment with 8.5 mg/kg of **10h** slightly reduced the volume of implanted prostatic tumors, treatment with 17 mg/kg of **10h** significantly inhibited the growth of implanted prostatic tumor ($P < 0.001$ vs the vehicle-treated control, Figure 5A and Figure 5B). More importantly, the tumor weights (0.5184 ± 0.1668 g, 0.2786 ± 0.1010 g) in the mice treated with **10h** at 8.5 mg/kg and 17 mg/kg were 30% and 62% (w/w) less than that in the vehicle-treated controls (0.7356 ± 0.1992 g, $P < 0.01$, Figure 5C) while the body weights of the mice were not significantly changed by treatment with **10h** (Figure 5D). Together, our data clearly demonstrated that **10h** inhibited the growth of implanted tumors in vivo and its anticancer activity tended to be dose-dependent.

*Treatment with **10h** Induces Prostatic Cancer Cell Cycling Arrest and Apoptosis.* To understand the mechanisms underlying the action of **10h**, the effects of **10h** on prostatic cancer cell cycling were examined. DU-145 cells were treated with different concentrations of **10h** (0.08 μM, 0.16 μM) and CDDO-Me (0.26 μM, 0.53 μM) for 24 h and stained with PI, followed by flow cytometry analysis (Figure 6A). As shown in Figure 6B, treatment with **10h** induced DU-145 cell cycle arrest at G_0/G_1 phase and the percentages of DU-145 cells at G0/G1 phase were 68% (0.16 μM **10h**) and 68% (0.53 μM CDDO-Me), respectively, which were significantly higher than that of

DOI: 10.1021/jm5020023
J. Med. Chem. XXXX, XXX, XXX−XXX

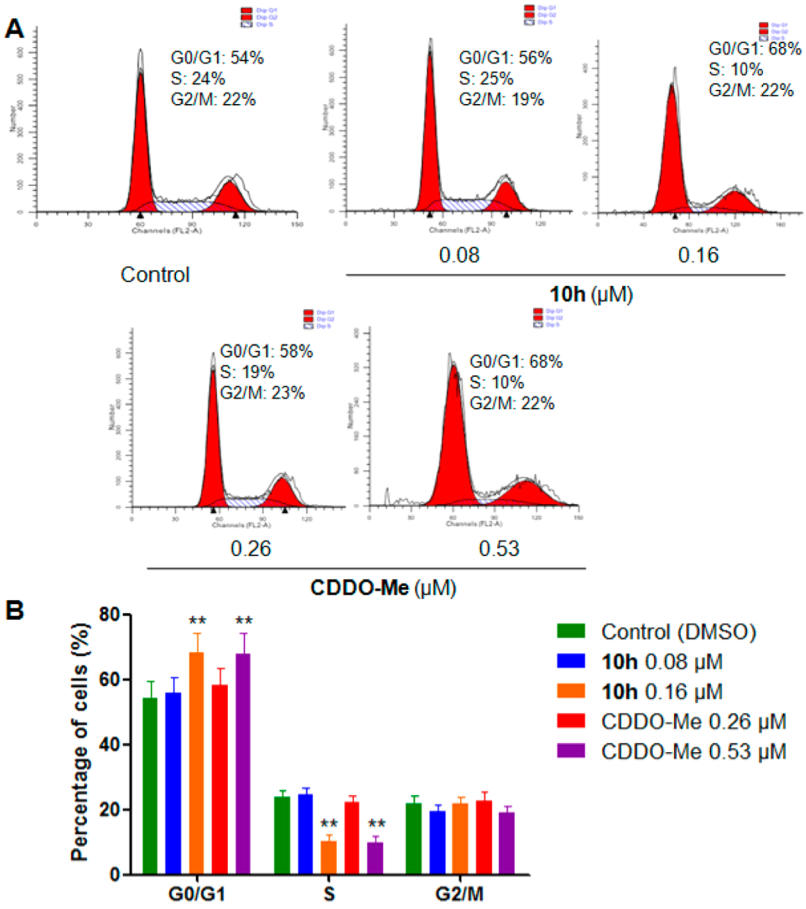

Figure 6. Effects of **10h** on cell-cycling of DU-145 cells. Cells were treated with the indicated concentrations of **10h** and CDDO-Me for 24 h and stained with PI, followed by flow cytometry analysis: (A) representative histograms; (B) quantitative analysis. Data are representative histograms and expressed as the mean ± SD of each compound from three independent experiments: (**) $P < 0.01$ vs the vehicle-treated controls.

vehicle-treated controls. As a result, the percentages of prostatic cancer cells at S phase in 0.16 μM **10h**-treated cells or 0.53 μM CDDO-Me-treated cells were significantly lower than those of vehicle-treated controls.

Tumor cells arrested at G0/G1 phase are associated with high sensitivity to apoptotic triggers. Next, the impact of **10h** on the apoptosis of DU-145 cells was examined by Hoechst 33258 staining. As shown in Figure 7A, the vehicle-treated prostatic cancer cells (0.1% DMSO) displayed weak homogeneous blue in the nuclei while the CDDO-Me (0.53 μM) and **10h** (0.08−0.32 μM) treated prostatic cancer cells exhibited bright chromatin condensation and nuclear fragmentation, a hallmark of apoptosis. In comparison with that of the vehicle-treated control DU-145 cells, treatment with 0.08, 0.16, or 0.32 μM **10h**, like with 0.53 μM CDDO-Me, significantly reduced the relative levels of BcL-2 expression, although the treatment did not alter the relative levels of Bax expression in DU-145 cells (Figure 7B). As a result, these treatments obviously increased the ratios of Bax to BcL-2, which was associated with cell apoptosis. In addition, these treatments also significantly increased the activity of caspase-3 in DU-145 cells (Figure 7C). These three independent lines of evidence indicated that treatment with **10h** induced prostatic cancer cell apoptosis.

*Treatment with **10h** Inhibits the AKT/mTOR Signaling in DU-145 Cells.* The PI3K/AKT/mTOR pathway is crucial for the growth of many types of tumors. Finally, we examined the impact of treatment with **10h** on the AKT and mTOR activation in DU-145 cells by Western blot assays. As shown in Figure 8, there was no significant difference in the relative levels of AKT and mTOR expression in the different groups of cells, indicating that treatment with either **10h** or CDDO-Me did not alter the levels of AKT and mTOR expression in DU-145 cells. Interestingly, treatment with CDDO-Me significantly reduced the relative levels of phosphorylated AKT and mTOR in DU145 cells, as compared with that in the vehicle-treated controls. Similarly, treatment with either dose of **10h** also significantly decreased the relative levels of AKT phosphorylation, and treatment with a higher dose of **10h** dramatically reduced the relative levels of phosphorylated mTOR in DU-145 cells. Therefore, **10h**, like CDDO-Me, inhibited spontaneous activation of the AKT/mTOR pathway in DU-145 cells, which might contribute to its pharmacological action in inhibiting the growth of implanted prostatic cancer in vivo.

*The log P, Stability and Caco2 Permeability of **10h**.* The log *P* values of each analogues were analyzed using three methods reported previously,[25−30] and they are shown in Table 6 and Table S1 in Supporting Information. Furthermore, we observed that following incubation with **10h** or CDDO-Me in rat plasma at 37 °C for 1 h, 46% of **10h** and 32% of CDDO-Me remained (Table 6), suggesting that **10h** may be more stable in rat plasma than CDDO-Me. Similarly, **10h** displayed a longer half-life than CDDO-Me (39 vs 21 min) in human liver microsomes (HLM) (Table 6).

In addition, we characterized the potential ring-opened products or adduct products by LC−MS/MS following incubation

DOI: 10.1021/jm5020023
J. Med. Chem. XXXX, XXX, XXX−XXX

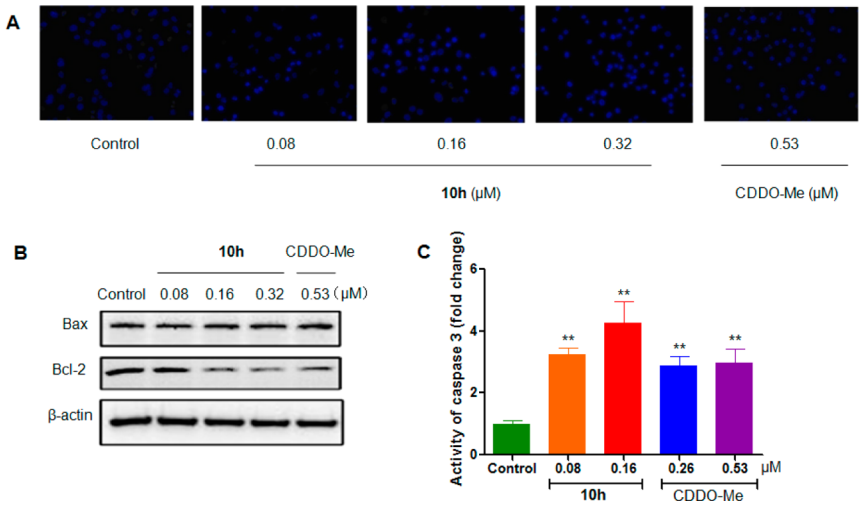

Figure 7. Effects of **10h** on induction of DU-145 cell apoptosis. DU-145 cells were treated with the indicated concentrations of compound or vehicle (control) for 24 h. The cells were stained with Hoechst 33258 and examined under a fluorescent microscope. Furthermore, the relative levels of Bax and BcL-2 as well as the levels of caspase 3 activity in the different groups of cells were determined by Western blot and enzymatic assays, respectively. Data are representative images and expressed as the mean ± SD of each group of cells from three separate experiments: (A) fluorescent staining of tumor cells; (B) Western blot analysis of the levels of Bax and BcL-2 expression; (C) levels of caspase-3 activity; (**) $P < 0.01$ vs the vehicle-treated control.

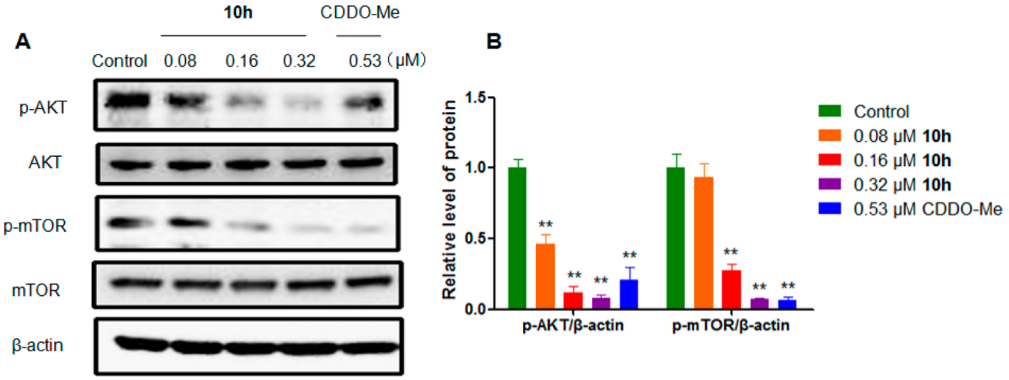

Figure 8. Effects of **10h** on the AKT/mTOR activation in DU-145 cells. DU-145 cells were treated with vehicle or the indicated compound for 24 h, and the relative levels of AKT and mTOR expression and phosphorylation were determined by Western blot assays using β-actin as a control. Data are representative images and expressed as the mean ± SD of each group of cells from three separate experiments: (A) Western blot analysis of the relative levels of AKT and mTOR expression and phosphorylation; (B) quantitative analysis; (**) $P < 0.01$ vs control.

Table 6. The log *P*, Rat Plasma Stability, Microsomal Stability, and Caco2 Permeability Data of 10h and CDDO-Me

		stability		Caco2 ($P_{app} \times 10^{-7}$ cm/s)[d]		
compd	log *P*[a]	1 h (%)[b]	$t_{1/2}$ (min)[c]	A to B	B to A	efflux ratio[e]
10h	6.7 ± 0.1	46 ± 3*[f]	39 ± 4*[f]	0.45 ± 0.21	0.59 ± 0.17	1.31
CDDO-Me	5.5 ± 0.3	32 ± 3	21 ± 2	1.42 ± 0.84	2.40 ± 1.45	1.69

[a]The log *P* values were calculated using the methods reported previously. Data are expressed as the mean ± SD from three different programs. [b]Rat plasma stability, the percentages of the tested compound remaining after incubations. [c]Half-life ($t_{1/2}$) in human liver microsomes. [d]Apparent permeability measured in Caco2 cells. "A to B" indicates the experiment from apical to basolateral, and "B to A" indicates the experiment from basolateral to apical. [e]Ratio BA/AB permeability coefficients. [f](*) $P < 0.05$ vs the CDDO-Me.

of **10h** with nucleophiles (Cys and GSH), in rat plasma, or human liver microsomes (HLM) at 37 °C for 1 h. As shown in Table S2, there were no detectable ring-opened products, although there were some adduct products following incubation of **10h** with the nucleophiles. These adduct products might stem from addition of the nucleophiles to ring A of **10h**, similar to that of CDDO-Me under the same conditions. These results suggest that γ-lactam ring of **10h** may be relatively stable in the rat plasma and HLM.

Next, the Caco2 permeability of **10h** was determined by the Caco2 bidirectional permeability assays. We found that the permeability data of **10h** ($P_{app,A\rightarrow B}$, from apical to basolateral direction) and ($P_{app,B\rightarrow A}$ from basolateral to apical direction) were 0.45×10^{-7} and 0.59×10^{-7} cm/s, respectively. The efflux ratio, defined as the ratio of $P_{app,B\rightarrow A}$ to $P_{app,A\rightarrow B}$, was 1.31 (Table 6). These data suggest that **10h** might not be a substrate of P-gp transporters, and it may possess a reasonable absorption rate in human intestine.

DOI: 10.1021/jm5020023
J. Med. Chem. XXXX, XXX, XXX−XXX

hERG Channel Inhibition. The human ether-a-go-go-related gene (hERG) codes the α subunit of a potassium ion channel (K_v11.1), and inhibition of the channel can result in long QT syndrome, a potential fetal disorder associated with severe adverse effect of drugs.[31] Accordingly, we tested the potential inhibition of **10h** on the hERG channel activity by the patch-clamp assay in Chinese hamster ovary (CHO) cells that were stably expressing the hERG channels. Notably, **10h** exhibited significantly lower hERG inhibitory activity (IC_{50} > 40 μM) than the control cisapride (IC_{50} = 0.04 μM), suggesting that **10h** may have little cardiac toxicity (Table 7).

Table 7. Inhibitory Activity of 10h on the hERG Channel by Patch-Clamp Assay

compd	hERG channel inhibition, IC_{50} (μM)[a]
10h	>40*[b]
cisapride	0.04

[a]Experiments were performed using Chinese hamster ovary (CHO) cells that had been stably transfected with the hERG. CHO cells were treated with different concentrations of **10h** (0.0128, 0.064, 0.32, 1.6, 8, and 40 μM) or the control cisapride (0.00096, 0.0048, 0.024, 0.12, 0.6, and 6 μM), and their whole-cell currents were recorded using an automated patch-clamp system (Qpatch). Data are expressed as the IC_{50} of each compound from three separate experiments. [b]No hERG inhibition detectable at the highest measured concentration (40 μM). (*) P < 0.001 vs cisapride.

CYP450 Inhibition of Selective Compounds. Drug-related adverse effects are a major challenge of drug development[32] and may be attributed to the inhibition or induction of members of the cytochrome P450 enzyme family.[33] To further evaluate the potential adverse effect of **10h**, the inhibition of **10h** on five major CYP450 enzymes was determined in human liver microsomes using CDDO-Me as a reference. As shown in Table 8, both **10h** and CDDO-Me had little inhibitory activity against CYP1A2 and CYP2D6 (IC_{50} > 100 μM) and medium to high inhibition on CYP2C19 and CYP3A4 (IC_{50} = 0.932−19.829 μM). In addition, **10h** had significantly lower inhibition on CYP2C9 (IC_{50} > 100 μM) than CDDO-Me (IC_{50} = 8.543 μM).

CONCLUSIONS

In summary, we have designed and synthesized a group of olean-28,13β-lactam compounds **10a−j**. This is the first report on the synthesis of γ-lactams from natural rigid polycyclic amides, promoted by an easily available reagent DDQ, through the intramolecular dehydrogenative C−N coupling reaction via a radical ion mechanism. We found that compound **10h** had potent and selective antiproliferative activity against several types of human cancer cells in vitro. Furthermore, **10h** showed a relatively lower acute toxicity in mice, and treatment with **10h** significantly inhibited the growth of implanted prostatic cancer in mice. In addition, treatment with **10h** induced prostatic cancer cell cycle arrest at G0/G1 phase and apoptosis in vitro, increased ratios of Bax to BcL-2 as well as decreased spontaneous activation of the AKT/mTOR pathway in DU-145 cells. Finally, **10h** was more stable in rat plasma and human liver microsomes than CDDO-Me and had little hERG channel inhibitory activity. These findings may provide a proof of principle that our novel and practical strategy for building of γ-lactam ring from natural rigid polycyclic amides may have broad applications in drug discovery and development field and that olean-28,13β-lactams may be potential chemotherapeutic agents for the intervention of prostate cancer.

EXPERIMENTAL PROTOCOLS

Chemical Analysis. Melting points were determined on a Mel-TEMP II melting point apparatus and were uncorrected. Infrared (IR) spectra (KBr) were recorded on a Nicolet Impact 410 instrument (KBr pellet). ^{1}H NMR and ^{13}C NMR spectra were recorded with a Bruker Avance 300 MHz spectrometer at 300 K, using TMS as an internal standard. MS spectra were recorded on a Mariner mass spectrometer (ESI) and high resolution mass spectrometry (HRMS) spectra on an Agilent Technologies LC/MSD TOF instrument. Analytical and preparative TLC was performed on silica gel (200−300 mesh) GF/UV 254 plates, and the chromatograms were visualized under UV light at 254 and 365 nm. All solvents were reagent grade and, when necessary, were purified and dried by standard methods. Solutions after reactions and extractions were concentrated using a rotary evaporator operating at a reduced pressure of ~20 Torr. The purity of all tested compounds was characterized by HPLC analysis (LC-10A HPLC system consisting of LC-10ATvp pumps and an SPD-10Avp UV detector). Individual compounds with a purity of >95% were used for subsequent experiments (see the Supporting Information). Oleanolic acid (OA) was commercially available. Compound **1** was prepared according to the method described previously.[11]

Benzyl 3β-Acetoxy-12-oxoolean-9(11)-en-28-oate (2). To a stirred solution of **1** (52.5 g, 87 mmol) in glacial acetic acid (100 mL) was added dropwise hydrobromic acid (4.4 mL, 38 mmol) at room temperature. The reaction mixture was then heated to 50 °C, and bromine (5.6 mL, 104 mmol) was thus added dropwise. The resulting reaction mixture was kept stirring for another 24 h. After completion of the reaction monitored by TLC, it was quenched by 20% aqueous sodium thiosulfate (100 mL) and then diluted with water (1.5 L) and filtered. The solid was washed with water, dried, and subjected to flash column chromatography over silica gel using petroleum ether/EtOAc (9:1) to give a yellowish solid **2** (42 g, 80%). Mp 216−218 °C. IR (KBr, cm^{-1}): 3410, 2954, 2873, 1733, 1652, 1465, 1385, 1368, 1329, 1242. ESI-MS: 603 [M + H]$^+$. ^{1}H NMR (300 M Hz, $CDCl_3$, 25 °C, TMS): δ 7.34−7.26 (m, 5H), 5.7 (s, 1H), 5.16 (d, J = 12.6 Hz, 1H), 5.11 (d, J = 12.6 Hz, 1H), 4.46−4.40 (m, 1H), 3.03−3.00 (m, 1H), 2.93 (d, J = 4.5 Hz, 1H), 2.05 (s, 3H), 2.01 (s, 3H), 1.57 (s, 3H), 1.16 (s, 3H), 1.00 (s, 3H), 0.95 (s, 3H), 0.92 (s, 3H), 0.89 (s, 3H) ppm. ^{13}C NMR (75 M Hz, $CDCl_3$, 25 °C, TMS): δ 200.2, 177.8, 177.5, 170.1, 136.4, 128.5, 128.5, 128.4, 128.4, 128.1, 122.8, 79.7, 66.1, 50.3, 49.4, 47.2, 45.2, 41.7, 39.8, 38.2, 36.1, 35.9, 34.6, 33.3, 32.9, 32.8, 31.6, 30.7, 28.0, 28.0, 23.9, 23.9, 23.5, 23.2, 22.8, 21.6, 21.2, 17.8, 16.7 ppm.

Benzyl 3β-Hydroxy-12-oxoolean-9(11)-en-28-oate (3). A solution of **2** (42 g, 70 mmol) and KOH (39 g, 0.7 mol) in MeOH

Table 8. CYP450 Inhibition by 10h and CDDO-Me

	human CYP450 inhibition (IC_{50}, μM)[a]					
compd	1A2	2C9	2C19	2D6	3A4 (M)[b]	3A4 (T)[c]
10h	>100	>100*[d]	8.107	>100	0.932	2.535
CDDO-Me	>100	8.543	19.829	>100	4.780	2.740

[a]IC_{50} refers to the concentration of a compound that causes 50% inhibition of the enzyme activity. [b]Midazolam was used as substrate. [c]Testosterone was used as substrate. [d](*) P < 0.01 vs CDDO-Me.

DOI: 10.1021/jm5020023
J. Med. Chem. XXXX, XXX, XXX−XXX

(100 mL) was heated under reflux for 45 min. After removal of MeOH in vacuum, the resulting mixture was acidified with aqueous HCl (6 M) solution. The aqueous layer was extracted with a mixture of CH_2Cl_2 and Et_2O (1:2) (three times). The combined organic layers were washed with saturated sodium hydrogen carbonate solution and brine and dried over magnesium sulfate. The solvent was removed to give an amorphous solid **3** (39 g, quantitative), which was used for the next reaction without further purification. An analytically pure sample was obtained by recrystallization from methanol. Mp 197−198 °C. IR (KBr, cm^{-1}): 3506, 2953, 2930, 2867, 1715, 1647, 1587, 1456, 1382, 1236. ESI-MS *m/z*: 561 $[M + H]^+$. ^1H NMR (300 M Hz, $CDCl_3$, 25 °C, TMS): δ 7.34−7.26 (m, 5H), 5.7 (s, 1H), 5.16 (d, J = 12.6 Hz, 1H), 5.11 (d, J = 12.6 Hz, 1H), 3.22−3.17 (m, 1H), 3.03−3.00 (m, 1H), 2.25 (d, J = 4.5 Hz, 1H), 1.14 (s, 3H), 1.02 (s, 3H), 1.00 (s, 3H), 0.96 (s, 3H), 0.92 (s, 3H), 0.89 (s, 3H), 0.81 (s, 3H) ppm. ^{13}C NMR (75 M Hz, $CDCl_3$, 25 °C, TMS): δ 200.4, 178.5, 177.5, 136.3, 128.5, 128.5, 128.4, 128.4, 128.1, 122.6, 77.8, 66.1, 50.2, 49.3, 47.2, 45.3, 41.7, 40.0, 39.3, 36.5, 35.9, 34.5, 33.3, 32.9, 32.8, 31.6, 30.7, 28.1, 28.0, 27.5, 23.8, 23.4, 23.2, 22.8, 21.7, 18.0, 15.7 ppm.

Benzyl 3,12-Dioxoolean-9(11)-en-28-oate (4). To a solution of **3** (39 g, 0.07 mol) in acetone (150 mL) in an ice bath was added Jones reagent dropwise until the color of the solution changed from green to pale brown. The mixture was stirred at room temperature for 10 min. After removal of acetone, water was added to quench the reaction. The aqueous mixture was extracted with a mixture of CH_2Cl_2 and Et_2O (1:2) (three times). The combined organic layers were washed with saturated sodium hydrogen carbonate solution and brine and dried over magnesium sulfate. The solvent was removed and the crude product was purified by column chromatography (PE/EtOAc = 6:1) to obtain **4** (34 g, 88%) as an amorphous solid. Mp 146−147 °C. IR (KBr, cm^{-1}): 3421, 2946, 2861, 2359, 1723, 1708, 1662, 1599, 1466, 1383. ESI-MS *m/z*: 559 $[M + H]^+$. ^1H NMR (300 M Hz, $CDCl_3$, 25 °C, TMS): δ 7.38−7.28 (m, 5H), 5.8 (s, 1H), 5.16 (d, J = 12.6 Hz, 1 H), 5.11 (d, J = 12.6 Hz, 1H), 3.06−3.00 (m, 1H), 2.78 (d, J = 4.5 Hz, 1H), 2.66−2.17 (m, 3H), 1.26 (s, 3H), 1.11 (s, 3H), 1.07 (s, 3H), 1.00 (s, 3H), 0.97 (s, 3H), 0.95 (s, 3H), 0.89 (s, 3H) ppm. ^{13}C NMR (75 M Hz, $CDCl_3$, 25 °C, TMS): δ 215.7, 199.9, 177.4, 176.6, 136.3, 128.5, 128.5, 128.4, 128.4, 128.2, 124.0, 50.9, 49.5, 47.5, 47.2, 45.4, 41.8, 39.4, 37.0, 35.9, 34.5, 34.2, 33.3, 32.8, 31.9, 31.6, 30.7, 29.7, 28.0, 26.3, 23.8, 23.3, 23.2, 22.8, 21.6, 21.4, 19.1 ppm.

Benzyl 2-Hydroxymethylene-3,12-dioxoolean-9(11)-en-28-oate (5). To a solution of **4** (34 g, 0.06 mol) in dry CH_2Cl_2 (100 mL) were added ethyl formate (97%) (18 g, 0.24 mol) and NaOMe (19.5 g, 0.36 mol). The mixture was stirred at room temperature for 2 h. Then the mixture was diluted with a mixture of CH_2Cl_2 and Et_2O (1:2) and washed with 5% aqueous HCl solution (three times). The washings were re-extracted with a mixture of CH_2Cl_2 and Et_2O (1:2), and the combined organic layers were washed with saturated sodium hydrogen carbonate solution and brine and dried over magnesium sulfate. The solvent was removed and the crude product was purified by column chromatography (PE/EtOAc = 5:1) to obtain **5** (31.5 g, 90%) as an amorphous solid. Mp 110−114 °C. IR (KBr, cm^{-1}): 3463, 2950, 2869, 1758, 1723, 1661, 1596, 1456, 1384, 1365. ESI-MS: 587 $[M + H]^+$. ^1H NMR (300 M Hz, $CDCl_3$, 25 °C, TMS): δ 14.85 (d, J = 2.4 Hz, 1H), 8.75 (s, 1H), 7.34−7.26 (m, 5H), 5.7 (s, 1H), 5.16 (d, J = 12.6 Hz, 1H), 5.11 (d, J = 12.6 Hz, 1H), 3.03−3.00 (m, 1H), 2.83 (d, J = 4.5 Hz, 1H), 2.61 (d, J = 14.4 Hz, 1H), 2.25 (d, J = 14.4 Hz, 1H), 1.24 (s, 3H), 1.15 (s, 3H), 1.14 (s, 3H), 1.01 (s, 3H), 0.98 (s, 3H), 0.94 (s, 3H), 0.85 (s, 3H) ppm. ^{13}C NMR (75 M Hz, $CDCl_3$, 25 °C, TMS): δ 200.0, 189.8, 188.3, 177.5, 175.7, 136.3, 128.6, 128.6, 128.5, 128.5, 128.2, 124.2, 105.0, 66.2, 49.5, 48.3, 47.2, 45.5, 42.3, 40.5, 39.1, 37.1, 36.0, 34.6, 33.3, 32.9, 31.6, 31.3, 30.7, 29.7, 28.3, 28.1, 23.4, 23.1, 22.8, 21.6, 20.8, 18.9 ppm.

Benzyl 12-Oxoisoxazolo[4,5-*b*]olean-9(11)-en-28-oate (6). To a solution of **5** (31 g, 53 mmol) in EtOH (110 mL) and water (10 mL) was added hydroxylamine hydrochloride (36.8 g, 530 mmol). The mixture was heated under reflux for 1 h. The mixture was concentrated in vacuo, and water (50 mL) was added. The mixture was extracted with EtOAc (three times). The combined organic layers were washed with water (three times) and saturated aqueous NaCl solution (three times), dried over $MgSO_4$, and filtered. The filtrate was evaporated in vacuo to give a solid. The solid was subjected to flash column chromatography (PE/EtOAc = 3:1) to give **6** as an amorphous solid (25.6 g, 83%). Mp 120−122 °C. IR (KBr, cm^{-1}): 3434, 2947, 2861, 2353, 2312, 1722, 1660, 1581, 1456, 1384. ESI-MS: 584 $[M + H]^+$. ^1H NMR (300 M Hz, $CDCl_3$, 25 °C, TMS): δ 8.05 (s, 1H), 7.34−7.26 (m, 5H), 5.8 (s, 1H), 5.16 (d, J = 12.6 Hz, 1H), 5.11 (d, J = 12.6 Hz, 1H), 3.10−3.00 (m, 1H), 2.80 (d, J = 4.5 Hz, 1H), 2.75 (d, J = 15 Hz, 1H), 3.38 (d, J = 15 Hz, 1H), 1.37 (s, 3H), 1.26 (s, 3H), 1.12 (s, 3H), 1.01 (s, 3H), 0.99 (s, 3H), 0.95 (s, 3H), 0.90 (s, 3H) ppm. ^{13}C NMR (75 M Hz, $CDCl_3$, 25 °C, TMS): δ 199.8, 177.4, 176.0, 172.1, 150.2, 136.3, 128.6, 128.6, 128.5,128.5, 128.1, 124.5, 108.6, 66.2, 49.8, 49.5, 47.2, 45.6, 41.8, 41.3, 36.0, 35.2, 34.6, 33.7, 33.3, 32.9, 31.6, 31.3, 30.7, 28.8, 28.2, 24.6, 23.2, 22.8, 22.8, 21.6, 21.4, 18.3 ppm.

12-Oxoisoxazolo[4,5-*b*]olean-9(11)-en-28-oate (7). Compound **6** (2 g, 3.4 mmol) was stirred under H_2 in the presence of 10% palladium carbon (0.4 g) in THF for 0.5 h. The mixture was filtered through a pad of Celite, and the filtrate was dried and concentrated to offer **7** as a white solid (1.5 g, 91%). Mp 224−226 °C. IR (KBr, cm^{-1}): 3455, 2939, 2867, 1706, 1659, 1632, 1478, 1454, 1384,1342. ESI-MS: 492 $[M - H]^-$. ^1H NMR (300 M Hz, $CDCl_3$, 25 °C, TMS): δ 8.05 (s, 1H), 5.8 (s, 1H), 3.03−3.00 (m, 1H), 2.93 (d, J = 4.5 Hz, 1H), 2.78 (d, J = 15.3 Hz, 1H), 2.40 (d, J = 15.3 Hz, 1H), 1.35 (s, 3H), 1.31 (s, 3H), 1.26 (s, 3H), 1.16 (s, 3H), 1.01 (s, 3H), 0.97 (s, 3H), 0.85 (s, 3H) ppm. ^{13}C NMR (75 M Hz, $CDCl_3$, 25 °C, TMS): δ 199.8, 183.8, 176.1, 172.1, 150.1, 124.5, 108.5, 49.7, 49.6, 47.1, 45.7, 41.8, 41.3, 35.8, 35.1, 34.5, 33.6, 33.2, 33.0, 31.4, 31.3, 30.6, 28.8, 28.2, 24.5, 23.1, 23.0, 22.6, 21.5, 21.4, 18.2 ppm.

General Procedure for the Preparation of 8a−j. A mixture of 7 (3.0 g, 6.1 mmol) and oxalyl chloride (5 mL) in anhydrous CH_2Cl_2 (50 mL) was stirred at room temperature overnight. The solvent was removed in vacuo, and the residue was coevaporated with anhydrous CH_2Cl_2 three times, and then used for the next reaction without further purification.

To a solution of the residue (178 mg, 0.35 mmol) obtained above in anhydrous CH_2Cl_2 (2 mL) was added a solution of primary amine (1.5 mmol). The mixture was stirred at room temperature overnight. The organic layer was separated and then diluted with CH_2Cl_2 (15 mL). It was washed with saturated sodium hydrogen carbonate solution and brine and dried over magnesium sulfate. The solvent was removed and the crude product was purified by flash column chromatography to obtain **8a−j** as an amorphous solid.

1-[12-Oxoisoxazolo[4,5-*b*]olean-9(11)-en-28-oyl]methylamide (8a). The title product was obtained in 70% yield as a white powder. Mp 175−177 °C. IR (KBr, cm^{-1}): 3128, 2971, 2867, 1658, 1526, 1400. ^1H NMR (300 M Hz, $CDCl_3$, 25 °C, TMS): δ 8.07 (s, 1H), 5.99−5.95 (m, 1H), 5.89 (s, 1H), 3.05 (d, J = 4.4 Hz, 1H), 2.90−2.76 (m, 5H), 2.44 (d, J = 15.1 Hz, 1H), 1.35 (s, 3H), 1.30 (s, 3H), 1.27 (s, 3H), 1.16 (s, 3H), 1.04 (s, 3H), 1.00 (s, 3H), 0.91 (s, 3H) ppm. ^{13}C NMR (75 M Hz, $CDCl_3$, 25 °C, TMS): δ 200.2, 177.8, 176.5, 172.0, 150.1, 124.3, 108.4, 49.6, 49.3, 46.6, 45.7, 41.7, 41.2, 36.2, 35.1, 34.6, 34.0, 33.5, 33.2, 32.0, 31.2, 30.6, 28.7, 28.0, 26.5, 24.5, 23.1, 23.1, 22.9, 21.7, 21.3, 18.2. ESI-MS: 529 $[M + Na]^+$.

1-[12-Oxoisoxazolo[4,5-*b*]olean-9(11)-en-28-oyl]ethylamide (8b). The title product was obtained in 67% yield as a white powder. Mp 155−157 °C. IR (KBr, cm^{-1}): 3128, 2971, 2867, 1658, 1526, 1400. ^1H NMR (300 M Hz, $CDCl_3$, 25 °C, TMS): δ 8.07 (s, 1H), 5.89−5.87 (m, 2H), 3.28−3.20 (m, 2H), 3.05 (d, J = 4.4 Hz, 1H), 2.87 (d, J = 13.1 Hz, 1H), 2.81 (d, J = 15.2 Hz, 1H), 2.43 (d, J = 15.0 Hz, 1H), 1.35 (s, 3H), 1.30 (s, 3H), 1.27 (s, 3H), 1.16 (s, 3H), 1.04 (s, 3H), 1.01 (s, 3H), 0.91 (s, 3H) ppm. ^{13}C NMR (75 M Hz, $CDCl_3$, 25 °C, TMS): δ 199.7, 176.4, 176.1, 171.6, 149.7, 123.9, 108.0, 49.1, 48.9, 46.0, 45.4, 41.3, 40.8, 35.8, 34.7, 34.1, 33.9, 33.6, 33.1, 32.8, 31.5, 30.8, 30.1, 28.3, 27.5, 24.1, 22.8, 22.6, 22.4, 21.3, 20.9, 17.8, 14.7. ESI-MS: 543 $[M + Na]^+$.

1-[12-Oxoisoxazolo[4,5-*b*]olean-9(11)-en-28-oyl]-*n*-propylamide (8c). The title product was obtained in 88% yield as a white powder. Mp 159−161 °C. IR (KBr, cm^{-1}): 3128, 2966, 2872, 1660, 1523, 1400. ^1H NMR (300 M Hz, $CDCl_3$, 25 °C, TMS): δ 8.07 (s, 1H),

DOI: 10.1021/jm5020023
J. Med. Chem. XXXX, XXX, XXX−XXX

5.94−5.89 (m, 2H), 3.27 (q, J = 6.4, 6.8 Hz, 2H), 3.05 (d, J = 4.2 Hz, 1H), 2.89 (d, J = 12.7 Hz, 1H), 2.81 (d, J = 15.1 Hz, 1H), 2.43 (d, J = 15.0 Hz, 1H), 1.35 (s, 3H), 1.30 (s, 3H), 1.27 (s, 3H), 1.16 (s, 3H), 1.04 (s, 3H), 1.01 (s, 3H), 0.91 (s, 3H) ppm. ^{13}C NMR (75 M Hz, $CDCl_3$, 25 °C, TMS): δ 199.7, 176.6, 176.1, 171.6, 149.7, 123.9, 108.0, 49.2, 48.9, 46.1, 45.3, 41.3, 40.8, 40.8, 35.8, 34.6, 34.1, 33.7, 33.1, 32.8, 31.5, 30.8, 30.1, 28.3, 27.5, 24.1, 22.8, 22.7, 22.6, 22.5, 21.3, 20.9, 17.8, 11.0. ESI-MS: 557 $[M + Na]^+$.

1-[12-Oxoisoxazolo[4,5-*b*]olean-9(11)-en-28-oyl]-*n*-butylamide (8d). The title product was obtained in 78% yield as a white powder. Mp 151−153 °C. IR (KBr, cm^{-1}): 3128, 2954, 2871, 1659, 1523, 1400. ^{1}H NMR (300 M Hz, $CDCl_3$, 25 °C, TMS): δ 8.07 (s, 1H), 5.95−5.89 (m, 1H), 5.89 (s, 1H), 3.28 (q, J = 6.4, 6.7 Hz, 2H), 3.06 (d, J = 4.4 Hz, 1H), 2.90 (d, J = 13.0 Hz, 1H), 2.82 (d, J = 15.1 Hz, 1H), 2.43 (d, J = 15.1 Hz, 1H), 1.35 (s, 3H), 1.30 (s, 3H), 1.27 (s, 3H), 1.17 (s, 3H), 1.04 (s, 3H), 1.01 (s, 3H), 0.91 (s, 3H) ppm. ^{13}C NMR (75 M Hz, $CDCl_3$, 25 °C, TMS): δ 199.7, 176.5, 176.0, 171.6, 149.8, 123.9, 108.0, 49.1, 48.9, 46.1, 45.3, 41.3, 40.8, 38.8, 35.8, 34.6 34.1, 33.7, 33.1, 32.8, 31.5, 31.4, 30.8, 30.1, 28.3, 27.5, 24.1, 22.8, 22.6, 22.5, 21.3, 20.9, 19.7, 17.8, 13.3. ESI-MS: 571 $[M + Na]^+$.

1-[12-Oxoisoxazolo[4,5-*b*]olean-9(11)-en-28-oyl]-*n*-hexylamide (8e). The title product was obtained in 69% yield as a white powder. Mp 142−144 °C. IR (KBr, cm^{-1}): 3129, 2932, 2860, 1600, 1524, 1399. ^{1}H NMR (300 M Hz, $CDCl_3$, 25 °C, TMS): δ 8.07 (s, 1H), 5.92−5.89 (m, 2H), 3.30 (q, J = 6.0, 7.0 Hz, 2H), 3.06 (d, J = 4.4 Hz, 1H), 2.89 (d, J = 13.1 Hz, 1H), 2.81 (d, J = 15.1 Hz, 1H), 2.43 (d, J = 15.0 Hz, 1H), 1.35 (s, 3H), 1.31 (s, 3H), 1.27 (s, 3H), 1.17 (s, 3H), 1.04 (s, 3H), 1.01 (s, 3H), 0.91 (s, 3H) ppm. ^{13}C NMR (75 M Hz, $CDCl_3$, 25 °C, TMS): δ 200.0, 176.9, 176.4, 172.0, 150.1, 124.4, 108.4, 49.6, 49.3, 46.5, 45.8, 41.8, 41.2, 39.6, 36.2, 35.1, 34.6, 34.1, 33.5, 33.2, 32.0, 31.4, 31.3, 30.6, 29.8, 28.7, 28.0, 26.6, 24.5, 23.3, 23.1, 23.0, 22.5, 21.7, 21.3, 18.2, 13.9. ESI-MS: 599 $[M + Na]^+$, 615 $[M + K]^+$.

1-[12-Oxoisoxazolo[4,5-*b*]olean-9(11)-en-28-oyl]-*tert*-butylamide (8f). The title product was obtained in 73% yield as a white powder. Mp 166−168 °C. IR (KBr, cm^{-1}): 3128, 2969, 2871, 1660, 1512, 1400. ^{1}H NMR (300 M Hz, $CDCl_3$, 25 °C, TMS): δ 8.07 (s, 1H), 5.88 (s, 1H), 5.53 (s, 1H), 3.10 (d, J = 4.3 Hz, 1H), 2.86−2.76 (m, 2H), 2.43 (d, J = 15.0 Hz, 1H), 1.35 (s, 3H), 1.29 (s, 3H), 1.27 (s, 3H), 1.17 (s, 3H), 1.03 (s, 3H), 1.00 (s, 3H), 0.90 (s, 3H) ppm. ^{13}C NMR (75 M Hz, $CDCl_3$, 25 °C, TMS): δ 199.5, 175.8, 175.6, 171.6, 149.7, 124.0, 108.0, 50.3, 49.2, 48.7, 46.2, 45.4, 41.3, 40.7, 35.8, 34.6, 34.2, 33.7, 33.1, 32.8, 31.5, 30.8, 30.1, 28.3, 28.3, 28.3, 28.3, 27.5, 24.0, 22.7, 22.7, 22.6, 21.2, 20.9, 17.8. ESI-MS: 571 $[M + Na]^+$.

1-[12-Oxoisoxazolo[4,5-*b*]olean-9(11)-en-28-oyl]ethoxylamide (8g). The title product was obtained in 90% yield as a white powder. Mp 162−164 °C. IR (KBr, cm^{-1}): 3129, 3009, 1655, 1620, 1400. ^{1}H NMR (300 M Hz, $CDCl_3$, 25 °C, TMS): δ 8.08 (s, 1H), 6.55 (m, 1H), 5.89 (s, 1H), 3.72−3.62 (m, 2H), 3.47−3.37 (m, 3H), 3.07−3.00 (m, 1H), 2.94 (d, J = 12.9 Hz, 1H), 2.81 (d, J = 15.0 Hz, 1H), 2.43 (d, J = 15.0 Hz, 1H), 1.35 (s, 3H), 1.32 (s, 3H), 1.27 (s, 3H), 1.17 (s, 3H), 1.04 (s, 3H), 1.00 (s, 3H), 0.91 (s, 3H) ppm. ^{13}C NMR (75 M Hz, $CDCl_3$, 25 °C, TMS): δ 199.9, 178.4, 176.3, 171.6, 149.7, 123.9, 108.0, 62.4, 49.1, 48.9, 46.2, 45.4, 42.2, 41.3, 40.8, 35.7, 34.7, 34.1, 33.6, 33.1, 32.8, 31.4, 30.8, 30.1, 28.3, 27.5, 24.1, 22.7, 22.6, 22.5, 21.3, 20.9, 17.7. ESI-MS: 559 $[M + Na]^+$.

1-[12-Oxoisoxazolo[4,5-*b*]olean-9(11)-en-28-oyl]cyclohexylamide (8h). The title product was obtained in 88% yield as a white powder. Mp 184−186 °C. IR (KBr, cm^{-1}): 2933, 2856, 1655, 1517, 1385. ^{1}H NMR (300 M Hz, $CDCl_3$, 25 °C, TMS): δ 8.07 (s, 1H), 5.89 (s, 1H), 5.65 (d, J = 7.9 Hz, 1H), 3.84−3.81 (m, 1H), 3.06 (d, J = 4.2 Hz, 1H), 2.88 (d, J = 13.3 Hz, 1H), 2.81 (d, J = 15.1 Hz, 1H), 2.43 (d, J = 15.1 Hz, 1H), 1.35 (s, 3H), 1.31 (s, 3H), 1.27 (s, 3H), 1.17 (s, 3H), 1.04 (s, 3H), 1.00 (s, 3H), 0.90 (s, 3H) ppm. ^{13}C NMR (75 M Hz, $CDCl_3$, 25 °C, TMS): δ 199.6, 175.9, 175.5, 171.6, 149.7, 123.9, 108.0, 49.1, 48.8, 47.5, 45.9, 45.4, 41.3, 40.8, 35.7, 34.6, 34.1, 33.7, 33.1, 32.8, 32.8, 32.7, 31.4, 30.8, 30.1, 28.3, 27.5, 25.0, 24.5, 24.5, 24.1, 22.9, 22.7, 22.5, 21.2, 20.9, 17.8. ESI-MS: 597 $[M + Na]^+$.

1-[12-Oxoisoxazolo[4,5-*b*]olean-9(11)-en-28-oyl]phenethylamide (8i). The title product was obtained in 68% yield as a white powder. Mp 151−153 °C. IR (KBr, cm^{-1}): 3132, 2972, 1656, 1520, 1400. ^{1}H NMR (300 M Hz, $CDCl_3$, 25 °C, TMS): δ 8.06 (s, 1H), 7.32−7.18 (m, 5H), 5.92 (t, J = 5.4 Hz, 1H), 5.87 (s, 1H), 3.58−3.49 (m, 2H), 2.97 (d, J = 4.4 Hz, 1H), 2.83−2.76 (m, 4H), 2.42 (d, J = 15.1, 1H), 1.34 (s, 3H), 1.26 (s, 3H), 1.19 (s, 3H), 1.15 (s, 3H), 1.10 (s, 3H), 1.00 (s, 3H), 0.96 (s, 3H) ppm. ^{13}C NMR (75 M Hz, $CDCl_3$, 25 °C, TMS): δ 199.5, 176.6, 175.9, 171.6, 149.7, 149.7, 138.4, 128.2, 128.2, 126.2, 126.2, 123.9, 108.0, 49.1, 48.8, 46.1, 45.3, 41.3, 40.7, 40.3, 35.7, 35.3, 34.6, 34.1, 33.6, 33.1, 32.8, 31.4, 30.7, 30.1, 28.3, 27.4, 24.1, 22.7, 22.6, 22.4, 21.2, 20.9, 17.7. ESI-MS: 619 $[M + Na]^+$.

1-[12-Oxoisoxazolo[4,5-*b*]olean-9(11)-en-28-oyl]phenylamide (8j). The title product was obtained in 60% yield as a white powder. Mp 157−159 °C. IR (KBr, cm^{-1}): 3135, 2950, 1655, 1522, 1400. ^{1}H NMR (300 M Hz, $CDCl_3$, 25 °C, TMS): δ 8.05 (s, 1H), 7.49−7.44 (m, 3H), 7.32 (t, J = 7.6, 8.2 Hz, 2H), 7.10 (t, J = 7.3 Hz,1H), 5.88 (s, 1H), 3.16 (d, J = 4.4 Hz, 1H), 3.00 (d, J = 12.7 Hz, 1H), 2.73 (d, J = 15.0, 1H), 2.36 (d, J = 15.0, 1H), 1.33 (s, 3H), 1.29 (s, 3H), 1.25 (s, 3H), 1.13 (s, 3H), 1.16 (s, 3H), 1.04 (s, 3H), 0.96 (s, 3H) ppm. ^{13}C NMR (75 M Hz, $CDCl_3$, 25 °C, TMS): δ 199.5, 176.6, 175.2, 171.8, 149.8, 137.4, 128.5, 128.5, 123.9, 123.9, 120.0, 120.0, 108.0, 49.1, 48.8, 47.0, 45.3, 41.3, 40.8, 35.7, 34.6, 34.1, 33.6, 33.2, 33.1, 31.6, 30.7, 30.2, 28.3, 27.4, 24.0, 22.8, 22.7, 22.7, 21.2, 20.9, 17.9. ESI-MS: 591 $[M + Na]^+$, 607 $[M + K]^+$.

General Procedure for the Preparation of the Mixture of Tautomers (9a−j). To a solution of **8a−j** (3.94 mmol) obtained above in MeOH (20 mL) and Et_2O (50 mL) in an ice bath was added NaOMe (7.25 g, 134 mmol). The mixture was stirred at room temperature for 45 min and then diluted with a mixture of CH_2Cl_2 and Et_2O (1:2). It was washed with 5% aqueous HCl solution (three times), and the acidic washings were reextracted with a mixture of CH_2Cl_2 and Et_2O (1:2). The combined organic layers were washed with saturated sodium hydrogen carbonate solution and brine and dried over magnesium sulfate. The solvent was removed to give a mixture of tautomers **9a−j** (quantitative). This material was used for the next reaction without further purification.

General Procedure for the Preparation of 10a−j. A mixture of **9a−j** (1 mmol) obtained above and DDQ (0.5 g, 2.2 mmol) in dry methylbenzene (4 mL) was heated to 80−110 °C for 8−24 h. After insoluble matter was removed by filtration, the filtrate was evaporated in vacuo to give a solid. The solid was subjected to flash column chromatography to give **10a−i** as an amorphous solid.

*Compound **10a**.* The title compound was obtained in 75% yield as a white powder. Mp 168−170 °C. IR (KBr, cm^{-1}): 3134, 2971, 2873, 1686, 1614, 1400. ^{1}H NMR (300 M Hz, $CDCl_3$, 25 °C, TMS): δ 7.98 (s, 1H), 5.85 (s, 1H), 2.78−2.60 (m, 4H), 1.47 (s, 3H), 1.26 (s, 3H), 1.17 (s, 3H), 1.01 (s, 3H), 0.98 (s, 3H), 0.88 (s, 3H), 0.85 (s, 3H) ppm. ^{13}C NMR (75 M Hz, $CDCl_3$, 25 °C, TMS): δ 198.7, 196.1, 177.2, 168.4, 165.3, 123.4, 114.1, 113.9, 87.0, 49.0, 47.2, 46.0, 45.4, 44.5, 42.1, 41.6, 35.6, 34.1, 33.5, 32.8, 31.6, 31.2, 30.1, 29.2, 27.3, 26.5, 24.3, 22.6, 22.4, 21.3, 21.1, 17.7. ESI-MS: 503 $[M + H]^+$, 525 $[M + Na]^+$. HRMS: calculated for $C_{32}H_{43}N_2O_3$ $[M + H]^+$ 503.3274, found 503.3281.

*Compound **10b**.* The title compound was obtained in 69% yield as a white powder. Mp 166−168 °C. IR (KBr, cm^{-1}): 3134, 2971, 2873, 1686, 1614, 1400. ^{1}H NMR (300 M Hz, $CDCl_3$, 25 °C, TMS): δ 8.00 (s, 1H), 5.85 (s, 1H), 3.14 (q, J = 7.1, 2H), 2.87 (t, J = 8.8, 1H), 1.45 (s, 3H), 1.28 (s, 3H), 1.25 (s, 3H), 1.15 (s, 3H), 1.04 (s, 3H), 1.01 (s, 3H), 0.99 (s, 3H) ppm. ^{13}C NMR (75 M Hz, $CDCl_3$, 25 °C, TMS): δ 201.5, 196.0, 165.2, 162.8, 160.8, 120.0, 114.3, 113.2, 85.5, 52.1, 51.4, 45.6, 45.2, 44.9, 39.7, 36.9, 36.7, 34.4, 34.0, 33.5, 33.4, 31.1, 27.7, 25.5, 24.3, 23.6, 23.0, 21.6, 21.1, 20.2, 20.2, 19.0, 15.5. ESI-MS: 517 $[M + H]^+$, 539 $[M + Na]^+$, 555 $[M + K]^+$. HRMS: calculated for $C_{33}H_{45}N_2O_3$ $[M + H]^+$ 517.3430, found 517.3416.

*Compound **10c**.* The title compound was obtained in 65% yield as a white powder. Mp 197−199 °C. IR (KBr, cm^{-1}): 3130, 2962, 1755, 1686, 1614, 1400. ^{1}H NMR (300 M Hz, $CDCl_3$, 25 °C, TMS): δ 7.95 (s, 1H), 5.86 (s, 1H), 3.10 (t, J = 7.2 Hz, 2H), 2.89 (t, J = 9.2, 1H), 1.47 (s, 3H), 1.25 (s, 3H), 1.15 (s, 3H), 1.01 (s, 3H), 0.98 (s, 3H), 0.88 (s, 3H), 0.85 (s, 3H) ppm. ^{13}C NMR (75 M Hz, $CDCl_3$, 25 °C, TMS): δ 196.4, 193.0, 173.1, 165.6, 164.1, 123.5, 115.0, 114.3, 87.0, 48.3, 47.9, 46.7, 45.1, 44.9, 42.9, 42.7, 36.7, 34.4, 34.0, 33.3, 32.8, 31.7,

DOI: 10.1021/jm5020023
J. Med. Chem. XXXX, XXX, XXX−XXX

30.7, 28.8, 27.6, 27.3, 25.9, 24.2, 23.8, 23.2, 22.1, 21.5, 20.1, 17.6. ESI-MS: 531 $[M + H]^+$. HRMS: calculated for $C_{34}H_{47}N_2O_3$ $[M + H]^+$ 531.3587, found 531.3591.

Compound ***10d***. The title compound was obtained in 60% yield as a white powder. Mp 111−113 °C. IR (KBr, cm^{-1}): 3129, 2928, 2857, 1751, 1686, 1400. ^1H NMR (300 M Hz, $CDCl_3$, 25 °C, TMS): δ 7.99 (s, 1H), 5.84 (s, 1H), 3.08−3.00 (m, 2H), 2.86 (t, J = 9.0 Hz, 1H), 1.48 (s, 3H), 1.25 (s, 3H), 1.14 (s, 3H), 1.00 (s, 3H), 0.97 (s, 3H), 0.87 (s, 3H), 0.85 (s, 3H) ppm. ^{13}C NMR (75 M Hz, $CDCl_3$, 25 °C, TMS): δ 200.0, 196.1, 177.2, 164.8, 160.3, 119.5, 113.8, 112.8, 88.6, 51.1, 51.0, 45.1, 44.8, 44.6, 44.4, 39.0, 36.3, 35.9, 33.6, 32.8, 32.6, 32.1, 31.4, 30.6, 29.2, 27.2, 25.8, 25.0, 23.2, 22.3, 20.6, 20.2, 20.1, 19.8, 18.7. ESI-MS: 545 $[M + H]^+$, 567 $[M + Na]^+$. HRMS: calculated for $C_{35}H_{49}N_2O_3$ $[M + H]^+$ 545.3743, found 545.3755.

Compound ***10e***. The title compound was obtained in 58% yield as a white powder. Mp 188−190 °C. IR (KBr, cm^{-1}): 3133, 2930, 2856, 1750, 1686, 1614, 1400. ^1H NMR (300 M Hz, $CDCl_3$, 25 °C, TMS): δ 7.95 (s, 1H), 5.84 (s, 1H), 3.06−3.00 (m, 2H), 2.89 (t, J = 9.2, 1H), 1.44 (s, 3H), 1.28 (s, 3H), 1.25 (s, 3H), 1.15 (s, 3H), 1.15 (s, 3H), 1.00 (s, 3H), 0.97 (s, 3H) ppm. ^{13}C NMR (75 M Hz, $CDCl_3$, 25 °C, TMS): δ 201.5, 196.0, 173.1, 165.2, 160.7, 120.0, 114.3, 113.2, 85.6, 52.1, 51.5, 45.6, 45.3, 45.2, 45.0, 36.9, 36.8, 34.5, 34.1, 33.5, 31.7, 31.1, 30.4, 29.7, 27.7, 27.2, 25.5, 24.3, 23.7, 23.0, 22.6, 21.7, 21.2, 20.3, 20.2, 19.0, 14.1. ESI-MS: 573 $[M + H]^+$, 595 $[M + Na]^+$. HRMS: calculated for $C_{37}H_{53}N_2O_3$ $[M + H]^+$ 573.4056, found 573.4072.

Compound ***10f***. The title compound was obtained in 60% yield as a white powder. Mp 179−181 °C. IR (KBr, cm^{-1}): 3128, 2927, 2862, 1671, 1521, 1452, 1391. ^1H NMR (300 M Hz, $CDCl_3$, 25 °C, TMS): δ 8.10 (s, 1H), 6.04 (s, 1H), 3.36 (d, J = 10.0, 1H), 1.48 (s, 3H), 1.25 (s, 3H), 1.20 (s, 3H), 1.17 (s, 3H), 1.15 (s, 3H), 1.05 (s, 3H), 0.96 (s, 3H) ppm. ^{13}C NMR (75 M Hz, $CDCl_3$, 25 °C, TMS): δ 203.5, 196.2, 175.7, 165.3, 163.8, 120.2, 114.5, 113.4, 77.5, 51.1, 50.7, 49.8, 48.5, 45.2, 43.4, 42.6, 41.6, 39.2, 34.0, 33.4, 33.0, 32.0, 31.3, 31.1, 29.9, 29.7, 29.3, 28.5, 26.2, 25.9, 25.2, 24.3, 21.4, 19.5, 14.1. ESI-MS: 567 $[M + Na]^+$, 583 $[M + K]^+$. HRMS: calculated for $C_{35}H_{48}N_2O_3Na$ $[M + Na]^+$ 567.3563, found 567.3551.

Compound ***10g***. The title compound was obtained in 55% yield as a white powder. Mp 145−147 °C. IR (KBr, cm^{-1}): 3130, 2997, 1673, 1608, 1400. ^1H NMR (300 M Hz, $CDCl_3$, 25 °C, TMS): δ 7.98 (s, 1H), 5.84 (s, 1H), 3.80−3.70 (m, 2H), 3.19 (t, J = 5.2 Hz, 2H), 2.88 (t, J = 8.9 Hz, 1H), 1.45 (s, 3H), 1.28 (s, 3H), 1.25 (s, 3H), 1.15 (s, 3H), 1.15 (s, 3H), 1.01 (s, 3H), 0.98 (s, 3H) ppm. ^{13}C NMR (75 M Hz, $CDCl_3$, 25 °C, TMS): δ 201.4, 195.9, 165.1, 162.8, 160.7, 120.0, 114.3, 113.3, 86.3, 62.3, 52.2, 51.5, 47.0, 45.5, 45.2, 45.0, 37.1, 36.8, 34.4, 34.1, 33.4, 31.1, 29.7, 27.5, 25.5, 24.4, 23.6, 22.9, 21.6, 21.2, 20.3, 20.2, 19.0. ESI-MS: 533 $[M + H]^+$, 555 $[M + Na]^+$, 571 $[M + K]^+$. HRMS: calculated for $C_{33}H_{44}N_2O_4Na$ $[M + Na]^+$ 555.3199, found 555. 3213.

Compound ***10h***. The title compound was obtained in 50% yield as a white powder. Mp 169−171 °C. IR (KBr, cm^{-1}): 3134, 2931, 2855, 1711, 1674, 1391. ^1H NMR (300 M Hz, $CDCl_3$, 25 °C, TMS): δ 8.05 (s, 1H), 6.22 (s, 1H), 3.47−3.20 (m, 1H), 2.79 (d, J = 13.1 Hz, 1H), 1.58 (s, 3H), 1.56 (s, 3H), 1.33 (s, 3H), 1.27 (s, 3H), 1.20 (s, 3H), 0.98 (s, 3H), 0.96 (s, 3H) ppm. ^{13}C NMR (75 M Hz, $CDCl_3$, 25 °C, TMS): δ 196.4, 193.2, 173.1, 165.6, 162.6, 123.6, 115.0, 114.2, 86.9, 54.8, 47.9, 46.6, 45.1, 44.8, 42.8, 42.7, 42.4, 36.8, 34.8, 34.4, 33.9, 33.3, 32.8, 31.7, 30.5, 28.9, 27.6, 27.3, 25.9, 25.7, 25.2, 25.0, 23.8, 23.2, 22.0, 21.5, 17.6. ESI-MS: 571 $[M + H]^+$, 593 $[M + Na]^+$. HRMS: calculated for $C_{37}H_{50}N_2O_3Na$ $[M + Na]^+$ 593.3719, found 593.3734.

Compound ***10i***. The title compound was obtained in 45% yield as a white powder. Mp 127−129 °C. IR (KBr, cm^{-1}): 3134, 2926, 1758, 1686, 1400. ^1H NMR (300 M Hz, $CDCl_3$, 25 °C, TMS): δ 7.96 (s, 1H), 7.27−7.01 (m, 5H), 5.83 (s, 1H), 3.39−3.30 (m, 2H), 2.88 (t, J = 8.9 Hz, 1H), 2.76−2.68 (m, 2H), 1.31 (s, 3H), 1.25 (s, 3H), 1.24 (s, 3H), 1.14 (s, 3H), 1.13 (s, 3H), 1.01 (s, 3H), 0.98 (s, 3H) ppm. ^{13}C NMR (75 M Hz, $CDCl_3$, 25 °C, TMS): δ 200.1, 196.8, 176.5, 164.6, 160.4, 128.3, 128.3, 128.2, 127.6, 127.6, 125.3, 119.5, 113.8, 112.7, 88.6, 51.1, 46.6, 44.8, 44.6, 39.0, 35.8, 33.7, 33.4, 32.8, 32.6, 30.6, 29.2, 27.2, 25.8, 25.0, 23.8, 23.0, 22.3, 21.0, 20.7, 20.2, 19.8, 19.5, 18.4. ESI-MS: 615 $[M + Na]^+$, 631 $[M + K]^+$. HRMS: calculated for $C_{39}H_{48}N_2O_3Na$ $[M + Na]^+$ 615.3563, found 615.3572.

Compound 12. A mixture of **8h** (50 mg, 0.087 mmol), DDQ (21.7 mg, 0.096 mmol), acetyl chloride (68 mg, 0.87 mmol), and triethylamine (17.0 mg, 0.174 mmol) in anhydrous toluene (2 mL) was reacted for 24 h. After filtration, the filtrate was evaporated in vacuo to give a residue, which was purified by flash column chromatography (petroleum ether/EtOAc) to give **12** as an amorphous solid (16.6 mg, 31%). Mp 98−100 °C. IR (KBr, cm^{-1}): 3449, 2931, 2361, 1789, 1638. ^1H NMR (300 M Hz, $CDCl_3$, 25 °C, TMS): δ 8.04 (s, 1H), 6.41 (d, J = 7.5 Hz, 1H), 5.53 (s, 1H), 3.77−3.78 (m, 1H), 2.79 (d, J = 15.2, 1H), 2.64−2.59 (m, 1H), 2.45 (d, J = 14.9, 1H), 1.34 (s, 3H), 1.25 (s, 3H), 1.22 (s, 3H), 1.17 (s, 3H), 1.11 (s, 3H), 0.92 (s, 3H), 0.90 (s, 3H) ppm. ^{13}C NMR (75 M Hz, $CDCl_3$, 25 °C, TMS): δ 176.3, 172.3, 169.7, 156.5, 149.6, 140.0, 129.2, 115.3, 108.5, 49.9, 48.6, 44.8, 43.1, 42.0, 40.7, 39.8, 34.5, 33.8, 33.6, 32.6, 32.4, 32.4, 32.1, 31.9, 30.2, 30.0, 28.4, 26.4, 25.3, 25.1, 25.0, 24.9, 23.1, 22.6, 20.8, 20.6, 20.2, 18.9,17.9. ESI-MS: 639 $[M + Na]^+$. HRMS: calculated for $C_{39}H_{56}N_2O_4Na$ $[M + Na]^+$ 639.4138, found 639.4149.

Compound 13h. A mixture of **8h** (100 mg, 0.174 mmol) obtained above and DDQ (39 mg, 0.174 mmol) in dry methylbenzene (4 mL) was heated to 90 °C for 10 h. After insoluble matter was removed by filtration, the filtrate was evaporated in vacuo to give a solid. The solid was subjected to flash column chromatography (petroleum ether/EtOAc) to give **13h** as a white powder (44 mg, 46%). Mp 157−159 °C. IR (KBr, cm^{-1}): 3140, 2931, 2855, 1711, 1674, 1400. ^1H NMR (300 M Hz, $CDCl_3$, 25 °C, TMS): δ 8.07 (s, 1H), 6.05 (s, 1H), 3.58−3.46 (m, 2H), 2.85 (d, J = 14.79 Hz, 1H), 2.58 (d, J = 14.79 Hz, 1H), 1.39 (s, 3H), 1.35 (s, 3H), 1.30 (s, 3H), 1.26 (s, 3H), 1.18 (s, 3H), 1.04 (s, 3H), 0.96 (s, 3H) ppm. ^{13}C NMR (75 M Hz, $CDCl_3$, 25 °C, TMS): δ 205.0, 175.8, 172.2, 150.2, 126.4, 121.4, 108.6, 83.4, 51.2, 50.9, 48.1, 48.0, 42.0, 41.9, 40.9, 39.1, 35.5, 35.4, 34.0, 33.4, 32.9, 32.8, 32.5, 32.4, 31.1, 30.6, 30.2, 29.7, 28.7, 26.4, 25.5, 24.9, 24.8, 24.2, 24.1, 21.5, 19.4. ESI-MS: 573 $[M + H]^+$, 595 $[M + Na]^+$. HRMS: calculated for $C_{37}H_{52}N_2O_3Na$ $[M + Na]^+$ 595.3876, found 595.3857.

Compound 15. A mixture of **14** (100 mg, 0.176 mmol) obtained above and DDQ (40 mg, 0.176 mmol) in dry methylbenzene (4 mL) was heated to 90 °C for 5 h. After insoluble matter was removed by filtration, the filtrate was evaporated in vacuo to give a solid. The solid was subjected to flash column chromatography (petroleum ether/EtOAc) to give **15** as a white powder (50 mg, 52%). Mp 134−136 °C. IR (KBr, cm^{-1}): 3136, 2941, 2840, 1711, 1660, 1398. ^1H NMR (300 M Hz, $CDCl_3$, 25 °C, TMS): δ 5.90 (s, 1H), 4.50−4.45 (m, 1H), 3.41 (d, J = 9.69 Hz, 1H), 1.41 (s, 3H), 1.34 (s, 3H), 1.19 (s, 3H), 1.04 (s, 3H), 0.95 (s, 3H), 0.93 (s, 3H), 0.89 (s, 3H) ppm. ^{13}C NMR (75 M Hz, $CDCl_3$, 25 °C, TMS): δ 205.2, 176.0, 173.6, 170.8, 119.8, 79.7, 79.7, 52.4, 52.4, 51.0, 50.6, 48.5, 42.7, 42.2, 40.5, 39.3, 38.6, 37.9, 34.1, 33.4, 33.1, 32.3, 31.1, 30.9, 30.3, 28.5, 28.5, 28.5, 27.8, 26.0, 24.3, 24.0, 23.5, 21.2, 19.1, 16.5. ESI-MS: 566 $[M + H]^+$, 588 $[M + Na]^+$. HRMS: calculated for $C_{36}H_{56}NO_4$ $[M + H]^+$ 566.4209, found 566.4196.

Measurement of Cell Proliferation. The impact of different compounds on cancer cell proliferation was tested by the CCK-8 method using a cell counting kit-8 (Dojindo Laboratories, Kumamoto, Japan), according to the manufacturer's instructions. Briefly, DU-145 (human prostate cancer cells), H460 (human non-small-cell lung cancer cells), Bxpc-3 (human pancreatic carcinoma cells), BEL-7404 (human hepatocellular carcinoma cells), and nontumor WPMY-1 (human prostatic stromal myofibroblast cells) at 5×10^3 cells/well were cultured overnight in 10% FCS DMEM in 96-well plates and treated in triplicate with 0.041−10 μM of each compound for 72 h. The cells in medium alone were used as controls, and medium alone was the background. During the last 30 min culture, individual wells were added with 10 μL of CCK-8 solution and the absorbance of the supernatants at 450 nm was measured in a microplate reader.

$$\text{inhibition (\%)} = \frac{A_{\text{control-background}} - A_{\text{treated-background}}}{A_{\text{control-background}}} \times 100$$

Acute Toxicity of 10h in Mice. Both genders of ICR mice at 7 weeks of age were purchased from SLACCAS (Shanghai, China) and

DOI: 10.1021/jm5020023
J. Med. Chem. XXXX, XXX, XXX−XXX

were housed in a specific pathogen free facility. The mice were randomly treated by gavage with a single dose of 800, 640, 512, 409.6, or 327.8 mg/kg of **10h** or vehicle control (n = 8 per group). The mice were monitored for their behaviors, the amounts of water and food consumption, body weights, and activity up to 14 days after treatment. The experimental protocols were evaluated and approved by the Ethics Committee of the China Pharmaceutical University.

Antitumor Effect of 10h in Mice. Individual male BALB/c nude mice (6−8 weeks, 18−22 g, SLACCAS) were implanted subcutaneously with 2×10^6 DU-145 cells in 0.1 mL of sterile saline on the right flank of the axillary region to induce solid tumors. When the tumor reached 100 ± 30 mm^3 in size, the mice were then randomly treated by gavage with the indicated dose of **10h** or the same volume of vehicle (1:1:8 of DMSO/Cremphor EL/PBS) daily for 21 consecutive days. The tumor volumes (TV) were measured every 3 days up to 21 days after initial treatment. The TV was calculated using the formula

$$\mathrm{TV} = \frac{\text{length} \times (\text{width})^2}{2}$$

Subsequently, the mice were sacrificed and the tumors were dissected out and weighed. The % tumor growth inhibition was determined as the tumor growth inhibition

$$\mathrm{TGI}\,(\%) = \left(1 - \frac{T}{C}\right) \times 100$$

where T is the mean tumor weight in treated group and C is the mean tumor weight in vehicle control group at the end point.

Cell Cycle Analysis. DU-145 cells were cultured in 10% FCS DMEM overnight and treated in triplicate with CDDO-Me (0.26 or 0.53 μM), compound **10h** (0.08 or 0.16 μM), or vehicle for 24 h. The cells were harvested, fixed with 70% ethanol for 2 h, and incubated with PI/RNase staining buffer (BD Pharmingen) for 15 min at room temperature. The DNA content in the different groups of cells was assessed by flow cytometry (FACSCalibur, Becton Dickinson, U.S.) and analyzed by the software MODFIT.

Hoechst 33258 Assay for Apoptosis. The impact of **10h** on DU-145 cell apoptosis was determined by Hoechst 33258 staining using the apoptosis Hoechst staining kit (catalog no. C1115, Beyotime Biotechnology, Jiangsu, China), according to the manufacturer's protocol. Briefly, DU-145 cells were treated with the indicated concentrations of **10h** and CDDO-Me for 24 h, fixed in 0.5 mL of methanol for 30 min, and stained with 1 mg/mL of Hoechst 33258, followed by examining under a fluorescent microscope.

Caspase-3 Activity Assay. Caspase-3 activity was assayed using a caspase-3 activity kit (catalog no. C1115, Beyotime Institute of Biotechnology, Haimen, Jiangsu, China), according to the manufacturere's protocol. This assay is based on the ability of caspase-3 to catalyze acetyl-Asp-Glu-Val-Asp p-nitroanilide into the yellow formazan product p-nitroaniline. DU-145 cells were treated with individual compounds, as described above, and harvested. After being washed with cold PBS, the cells were lyzed in lysis buffer (100 μL per 2×10^6 cells) on ice for 15 min and then centrifuged at 18 000g at 4 °C for 10 min. The cell lysates were tested for their caspase-3 activity by mixing 10 μL of individual cell lysates with 10 μL caspase-3 substrate (Ac-DEVD-pNA, 2 mM) in 80 μL of reaction buffer in triplicate at 37 °C for 2 h. The caspase-3 activity in individual samples was calculated based on the absorbance at 405 nm and was expressed as the relative percentage of enzyme activity to the control.

Western Blotting Assay. DU-145 cells (5×10^5/well) were cultured in 10% FCS Ham's F-12K medium in six-well plates overnight, and the cells were treated in duplicate with vehicle alone or the indicated compounds for 24 h. The cells were harvested and lysed in lysis buffer [50 mM Tris-HCl, pH 8, 5 mM EGTA, 150 mM NaCl, 0.5% Nonidet P-40, 0.5% Triton X-100], followed by centrifuging at 14 000g for 10 min at 4 °C. After quantification of protein concentrations using the BCA assay (Pierce BCA protein assay kit, product no. 23225), the cell lysate samples (50 μg/lane) were separated on 10−14% SDS−polyacrylamide gel and transferred to nitrocellulose membranes. After being blocked with 5% fat-free dried milk in 10 mM Tris-HCl (pH 8.0), 150 mM NaCl, 0.05% Tween 20 (TPBS) overnight at 4 °C, the membranes were incubated with anti-AKT (1:1000, Cell Signaling Technology, no. 9272), anti-mTOR (FRAP, 1:1000, SantaCruz Biotechnology, SC-1549), anti-β-actin (1:1000, Boxter, BM0627), antiphosphorylated AKT (Ser473, 1:1000, Santa Cruz Biotechnology, SC-7985-R), or anti-phospho-mTOR (Ser2448) (1:1000, Cell Signaling Technology, no. 2971), anti-Bax (P-19, 1:1000, Santa Cruz Biotechnology, SC-526), anti-Bcl-2 (C-2,1:1000, Santa Cruz, Biotechnology). The bound antibodies were detected by HRP-conjugated secondary antibodies, and immune complexes were visualized using enhanced chemiluminescence reagent from Thermo Fisher Scientific (Rockford, IL, USA). The relative levels of target proteins to the control were determined by densimetric analysis using AlphaEase FC (Alpha Innotech, USA) image analysis software.

log *P* Calculations. The log P values of each compound were determined theoretically using three different programs,[25] and the data are presented as the mean log P and standard deviation. These programs included ChemAxon's MarvinSketch,[26,27] Molinspiration software,[28] and VCCLAB's ALOGPS software.[29,30]

Rat Plasma Stability Assay.[34,35] Compound **10h** or CDDO-Me (50 ng/mL) was incubated with rat plasma (pooled, heparinized) at 37 °C for 60 min. The reactions were stopped by precipitation of plasma proteins with 5 volumes of cold acetonitrile containing an internal standard, and the concentrations of remaining compound were analyzed by LC−MS/MS.

Microsomal Stability Assay.[36,37] Human liver microsomes (HLMs) were diluted with potassium phosphate−$MgCl_2$ buffer (100 mM, pH 7.4) to a final protein concentration of 0.2 mg/mL. The HLMs were incubated with each compound (5 μM) in the presence of NADPH system at 37 °C for 0, 5, 10, 15, 30, or 60 min and quenched with acetonitrile, followed by centrifuged at 4000g for 15 min. The content of each compound in the supernatants was determined for its half-life ($t_{1/2}$) by LC−MS/MS analysis.

Caco2 Permeability Assay.[38−42] Caco2 cells between passages 20 and 40 were cultured at 37 °C in a 5% CO_2 and 90% relative humidity environment. After 21 days of culture, the integrity of the cell monolayer was verified by measuring the trans-epithelial electrical resistance (TEER). The drug transport from the apical side to the basolateral side (A−B) or from the basolateral side to the apical side was measured under the same conditions. The monolayer of cells was treated in triplicate with 0.5 μM of the tested drug in the well with the appropriate pH (pH 6.8 for apical side and pH 7.4 for basolateral side) at 37 °C for 30 min. Samples were collected from the donor and receiver sides at 0 and 5 min postincubation. The concentrations of the drug were determined by LC−MS/MS. The apparent permeability values (P_{app}) were calculated according to the equation,

$$P_{app} = \frac{dQ/dt}{AC_0}$$

where dQ/dt is the slope of the cumulative amount transported during the study period, A is the area of the insets, and C_0 is the starting concentration. For bidirectional permeability, the efflux ratio (ER) was defined as $P_{app(B\rightarrow A)}/P_{app(A\rightarrow B)}$, where A → B is apical to basolateral transport and B → A is basolateral to apical transport. A high efflux ratio (>3) indicates that a compound may be a substrate for P-gp or other active transport systems.

hERG Channel Inhibition Assay.[43−48] Chinese hamster ovary (CHO) cells stably expressing the hERG channel were cultured in DMEM/F-12, GlutaMAX with 10% fetal bovine serum, 100 units/mL penicillin, 100 μg/mL streptomycin, 1% Geneticin, and 10 μM HEPES at 37 °C in a humidified atmosphere of 5% CO_2. When the cells reached 60−80% confluency, the cells were harvested and placed on the Qstirrer in serum-free media for ∼30 min.

The extracellular Ringer's solution (2 mM $CaCl_2$, 1 mM $MgCl_2$, 10 mM HEPES, 4 mM KCl, 145 mM NaCl, 10 mM glucose, pH 7.40, adjusted with NaOH, 305 mOsm) and intracellular Ringer's solution (5.374 mM $CaCl_2$, 1.75 mM $MgCl_2$, 120 mM KCl, 10 mM HEPES, 5 mM EGTA, 4 mM Na-ATP, pH 7.25, adjusted with KOH,

DOI: 10.1021/jm5020023
J. Med. Chem. XXXX, XXX, XXX−XXX

290 mOsm) containing 4 mM Na2-ATP were used for measuring the whole-cell currents using a QPatch system (Sophion) in response to continuously executed voltage protocols, according to the manufacturer's recommendations. Upon onset of the voltage protocol, the cells were maintained at a holding potential (V_h) of −80 mV, clamped briefly to −50 mV (50 ms), depolarized to 20 mV for 5000 ms, and finally repolarized to −50 mV for 5000 ms, at which potential, the peak outward tail current was measured. Finally, the voltage returned to V_h for 3100 ms. Thus, voltage protocols were repeated every 15 s. For each cell, extracellular solution was applied prior to increasing concentrations of the tested compound.

Inhibition of Hepatic CYP Enzymes. Inhibition of each drug on metabolizing CYP enzymes was determined using recombinant human CYP enzymes (CYP1A2, CYP2C9, CYP2C19, CYP2D6, and CYP3A4).[49−52] Individual CYP enzymes reacted with their substrates at a final concentration approximating their K_m (phenacetin, 60 μM; diclofenac, 6 μM; smephenytoin, 20 μM; dextromethorphan, 5 μM; midazolam, 8 μM; testosterone, 50 μM) in the presence or absence of nine concentrations of each compound up to 1000 nM in duplicate for 1 h. The reactions were quenched with acetonitrile, and after being centrifuged, the content of probe metabolites in the supernatants was determined by LC−MS/MS. Amounts of metabolites produced were normalized to vehicle controls, and IC_{50} values of each compound for individual CYP enzymes were calculated using GraphPad Prism 5.0.

■ ASSOCIATED CONTENT

Ⓢ Supporting Information

Compound purity measured by HPLC, log *P* of selective compounds, possible metabolic products of **10h** and CDDO-Me, and a csv file containing molecular formula strings. The Supporting Information is available free of charge on the ACS Publications website at DOI: 10.1021/jm5020023.

■ AUTHOR INFORMATION

Corresponding Authors

*Z.H.: phone, +86-25-83271072; e-mail, cpudahuang@163.com.
*H.J.: phone, +86-25-86021369; fax, +86-25-86635503; e-mail, huijicpu@163.com.
*Y.Z.: phone, +86-25-83271015; fax, +86-25-83271015; e-mail, zyhtgd@163.com.

Author Contributions

‖Y.A. and Y.H. contributed equally to this work.

Notes

The authors declare no competing financial interest.

■ ACKNOWLEDGMENTS

This study was supported by grants from the National Natural Science Foundation of China (Grants 81273378, 21372261, 81202408, and 21472244) and the Project Program of State Key Laboratory of Natural Medicines, China Pharmaceutical University (Grants ZJ12020 and SKLNMZZCX201403).

■ ABBREVIATIONS USED

CDDO-Me, methyl-2-cyano-3,12-dioxooleana-1,9(11)-dien-28-oate; CDDO-MA, 1-[2-cyano-3,12-dioxooleana-1,9(11)-dien-28-oyl]-methylamide; CDDO-Im, 1-[2-cyano-3,12-dioxooleana-1,9(11)-dien-28-oyl]imidazole; PI3K, phosphoinositide 3-kinase; AKT, protein kinase B, a serine/threonine protein kinase; mTOR, mammalian target of rapamycin; PBS, phosphate buffered saline; SD, standard deviation; HPLC, high-performance liquid chromatography; DMSO, dimethyl sulfoxide; PE, petroleum ether; LD_{50}, dose that is lethal in 50% of test subjects; TMS, tetramethylsilane; UV, ultraviolet; w/w, weight per unit weight (weight-to-weight ratio); Bn, benzyl; QT, the length of time between the start of the Q wave and end of the T wave on an electrocardiogram; CYP, cytochrome P450 enzyme; HEPES, *N*-2-hydroxyethylpiperazine-*N*′-2-ethanesulfonic acid; EGTA, ethylene glycol bis(β-aminoethyl ether)-*N*,*N*,*N*′,*N*′-tetraacetic acid

■ REFERENCES

(1) Sporn, M. B.; Liby, K. T.; Yore, M. M.; Fu, L.; Lopchuk, J. M.; Gribble, G. W. New synthetic triterpenoids: potent agents for prevention and treatment of tissue injury caused by inflammatory and oxidative stress. *J. Nat. Prod.* **2011**, *74*, 537−545.

(2) Honda, T.; Rounds, B. V.; Bore, L.; Finlay, H. J., Jr.; Favaloro, F. G.; Suh, N.; Wang, Y.; Sporn, M. B.; Gribble, G. W. Synthetic oleanane and ursane triterpenoids with modified rings A and C: a series of highly active inhibitors of nitric oxide production in mouse macrophages. *J. Med. Chem.* **2000**, *43*, 4233−4246.

(3) Honda, T.; Honda, Y., Jr.; Favaloro, F. G.; Gribble, G. W.; Suh, N.; Place, A. E.; Rendi, M. H.; Sporn, M. B. A novel dicyanotriterpenoid, 2-cyano-3,12-dioxooleana-1,9(11)-dien-28-onitrile, active at picomolar concentrations for inhibition of nitric oxide production. *Bioorg. Med. Chem. Lett.* **2002**, *12*, 1027−1030.

(4) Liby, K. T.; Yore, M. M.; Sporn, M. B. Triterpenoids and rexinoids as multifunctional agents for the prevention and treatment of cancer. *Nat. Rev. Cancer* **2007**, *7*, 357−369.

(5) Liby, K. T.; Sporn, M. B. Synthetic oleanane triterpenoids: multifunctional drugs with a broad range of applications for prevention and treatment of chronic disease. *Pharmacol. Rev.* **2012**, *64*, 972−1003.

(6) Hong, D. S.; Kurzrock, R.; Supko, J. G.; He, X.; Naing, A.; Wheler, J.; Lawrence, D.; Eder, J. P.; Meyer, C. J.; Ferguson, D. A.; Mier, J.; Konopleva, M.; Konoplev, S.; Andreeff, M.; Kufe, D.; Lazarus, H.; Shapiro, G. I.; Dezube, B. J. A phase I first-in-human trial of bardoxolone methyl in patients with advanced solid tumors and lymphomas. *Clin. Cancer Res.* **2012**, *18*, 3396−3406.

(7) Chen, L.; Zhang, Y.; Kong, X.; Lan, E.; Huang, Z.; Peng, S.; Kaufman, D. L.; Tian, J. Design, synthesis, and antihepatocellular carcinoma activity of nitric oxide releasing derivatives of oleanolic acid. *J. Med. Chem.* **2008**, *51*, 4834−4838.

(8) Huang, Z.; Zhang, Y.; Zhao, L.; Jing, Y.; Lai, Y.; Zhang, L.; Guo, Q.; Yuan, S.; Zhang, J.; Chen, L.; Peng, S.; Tian, J. Synthesis and antihuman hepatocellular carcinoma activity of new nitric oxide-releasing glycosyl derivatives of oleanolic acid. *Org. Biomol. Chem.* **2010**, *8*, 632−639.

(9) Huang, Z.; Fu, J.; Liu, L.; Sun, Y.; Lai, Y.; Ji, H.; Knaus, E. E.; Tian, J.; Zhang, Y. Glycosylated diazeniumdiolate-based oleanolic acid derivatives: Synthesis, in vitro and in vivo biological evaluation as antihuman hepatocellular carcinoma agents. *Org. Biomol. Chem.* **2012**, *10*, 3882−3891.

(10) Fu, J.; Liu, L.; Huang, Z.; Lai, Y.; Ji, H.; Peng, S.; Tian, J.; Zhang, Y. Hybrid molecule from O^2-(2,4-dinitrophenyl)diazeniumdiolate and oleanolic acid: a GSTπ activated NO prodrug with selective antihuman hepatocellular carcinoma activity and improved stability. *J. Med. Chem.* **2013**, *56*, 4641−4655.

(11) Ding, Y.; Huang, Z.; Yin, J.; Lai, Y.; Zhang, S.; Zhang, Z.; Fang, L.; Peng, S.; Zhang, Y. DDQ-promoted dehydrogenation from natural rigid polycyclic acids or flexible alkyl acids to generate lactones by a radical ion mechanism. *Chem. Commun.* **2011**, *47*, 9495−9497.

(12) Zhang, Z.; Zhang, C.; Ding, Y.; Zhao, Q.; Yang, L.; Ling, J.; Liu, L.; Ji, H.; Zhang, Y. The activation of p38 and JNK by ROS, contribute to OLO-2-mediated intrinsic apoptosis in human hepatocellular carcinoma cells. *Food Chem. Toxicol.* **2014**, *63*, 38−47.

(13) Fenical, W.; Jensen, P. R.; Palladino, M. A.; Lam, K. S.; Lloyd, G. K.; Potts, B. C. Discovery and development of the anticancer agent salinosporamide A (NPI-0052). *Bioorg. Med. Chem.* **2009**, *17*, 2175−2180.

(14) Feling, R. H.; Buchanan, G. O.; Mincer, T. J.; Kauffman, C. A.; Jensen, P. R.; Fenical, W. Salinosporamide A: a highly cytotoxic proteasome inhibitor from a novel microbial source, a marine-

DOI: 10.1021/jm5020023
J. Med. Chem. XXXX, XXX, XXX−XXX

bacterium of the new genus *Salinospora*. *Angew. Chem., Int. Ed.* **2003**, *42*, 355−357.
(15) Wilson, M. C.; Nam, S.-J.; Gulder, T. A. M.; Kauffman, C. A.; Jensen, P. R.; Fenical, W.; Moore, B. S. Structure and biosynthesis of the marine Streptomycete Ansamycin Ansalactam A and its distinctive branched chain polyketide extender unit. *J. Am. Chem. Soc.* **2011**, *133*, 1971−1977.
(16) Okazaki, Y.; Ishizuka, A.; Ishihara, A.; Nishioka, T.; Iwamura, H. New dimeric compounds of avenanthramide phytoalexin in oats. *J. Org. Chem.* **2007**, *72*, 3830−3839.
(17) Guntern, A.; Ioset, J. R.; Queiroz, E. F.; Sandor, P.; Foggin, C. M.; Hostettmann, K. Heliotropamide, a novel oxopyrrolidine-3-carboxamide from *Heliotropium ovalifolium*. *J. Nat. Prod.* **2003**, *66*, 1550−1553.
(18) Omura, S.; Fujimoto, T.; Otoguro, K.; Matsuzaki, K.; Moriguchi, R.; Tanaka, H.; Sasaki, Y. Lactacystin, a novel microbial metabolite, induces neuritogenesis of neuroblastoma cells. *J. Antibiot.* **1991**, *44*, 113−116.
(19) Fenteany, G.; Standaert, R. F.; Lane, W. S.; Choi, S.; Corey, E. J.; Schreiber, S. L. Inhibition of proteasome activities and subunit-specific amino-terminal threonine modification by lactacystin. *Science* **1995**, *268*, 726−731.
(20) Manam, R. R.; Teisan, S.; White, D. J.; Nicholson, B.; Grodberg, J.; Neuteboom, S. T. C.; Lam, K. S.; Mosca, D. A.; Lloyd, G. K.; Potts, B. C. M. Lajollamycin , a nitro-tetraene spiro-β-lactone-γ-lactam antibiotic from the marine actinomycete *Streptomyces nodosus*. *J. Nat. Prod.* **2005**, *68*, 240−243.
(21) Choi, E.; Lee, C.; Cho, M.; Seo, J. J.; Yang, J. S.; Oh, S. J.; Lee, K.; Park, S. K.; Kim, H. M.; Kwon, H. J.; Han, G. Property-based optimization of hydroxamate-based γ-lactam HDAC inhibitors to improve their metabolic stability and pharmacokinetic profiles. *J. Med. Chem.* **2012**, *55*, 10766−10770.
(22) Duffy, R. A.; Morgan, C.; Naylor, R.; Higgins, G. A.; Varty, G. B.; Lachowicz, J. E.; Parker, E. M. Rolapitant (SCH 619734): A potent, selective and orally active neurokinin NK1 receptor antagonist with centrally-mediated antiemetic effects in ferrets. *Pharmacol., Biochem. Behav.* **2012**, *102*, 95−100.
(23) Yang, Z. Q.; Shu, Y.; Ma, L.; Wittmann, M.; Ray, W. J.; Seager, M. A.; Koeplinger, K. A.; Thompson, C. D.; Hartman, G. D.; Bilodeau, M. T.; Kuduk, S. D. Discovery of naphthyl-fused 5-membered lactams as a new class of M1 positive allosteric modulators. *ACS Med. Chem. Lett.* **2014**, *5*, 604−608.
(24) Kazmierski, W. M.; Andrews, W.; Furfine, E.; Spaltenstein, A.; Wright, L. Discovery of potent pyrrolidone-based HIV-1 protease inhibitors with enhanced drug-like properties. *Bioorg. Med. Chem. Lett.* **2004**, *14*, 5689−5692.
(25) Aksenov, A. V.; Smirnov, A. N.; Magedov, I. V.; Reisenauer, M. R.; Aksenov, N. A.; Aksenova, I. V.; Pendleton, A. L.; Nguyen, G.; Johnston, R. K.; Rubin, M.; De Carvalho, A.; Kiss, R.; Mathieu, V.; Lefranc, F.; Correa, J.; Cavazos, D. A.; Brenner, A. J.; Bryan, B. A.; Rogelj, S.; Kornienko, A.; Frolova, L. V. Activity of 2-aryl-2-(3-indolyl)acetohydroxamates against drug-resistant cancer cells. *J. Med. Chem.* **2015**, *58*, 2206−2220.
(26) *MarvinSketch: Marvin*, version 6.3.0; ChemAxon: Budapest, Hungary, 2014; http://www.chemaxon.com.
(27) Klopman, G.; Li, J.-Y.; Wang, S.; Dimayuga, M. Computer automated log P calculations based on an extended group contribution approach. *J. Chem. Inf. Comput. Sci.* **1994**, *34*, 752−781.
(28) Interactive log *P* calculator. Molinspiration Cheminformatics. www.molinspiration.com, 2014.
(29) Tetko, I. V.; Gasteiger, J.; Todeschini, R.; Mauri, A.; Livingstone, D.; Ertl, P.; Palyulin, V. A.; Radchenko, E. V.; Zefirov, N. S.; Makarenko, A. S.; Tanchuk, V. Y.; Prokopenko, V. V. Virtual computational chemistry laboratory—design and description. *J. Comput.-Aided Mol. Des.* **2005**, *19*, 453−463.
(30) ALOGPS; VCCLAB. Virtual Computational Chemistry Laboratory. http://www.vcclab.org, 2005.
(31) Fermini, B.; Fossa, A. A. The impact of drug-induced QT interval prolongation on drug discovery and development. *Nat. Rev. Drug Discovery* **2003**, *2*, 439−447.
(32) Kola, I.; Landis, J. Can the pharmaceutical industry reduce attrition rates? *Nat. Rev. Drug Discovery* **2004**, *3*, 711−715.
(33) Guengerich, F. P. Cytochrome p450 and chemical toxicology. *Chem. Res. Toxicol.* **2008**, *21*, 70−83.
(34) Zhu, W.; Hu, Q.; Hanke, N.; van Koppen, C. J.; Hartmann, R. W. Potent 11β-hydroxylase inhibitors with inverse metabolic stability in human plasma and hepatic S9 fractions to promote wound healing. *J. Med. Chem.* **2014**, *57*, 7811−7817.
(35) Emmerich, J.; Hu, Q.; Hanke, N.; Hartmann, R. W. Cushing's syndrome: development of highly potent and selective CYP11B1 inhibitors of the (pyridylmethyl)pyridine type. *J. Med. Chem.* **2013**, *56*, 6022−6032.
(36) Lin, X.; Chen, W.; Qiu, Z.; Guo, L.; Zhu, W.; Li, W.; Wang, Z.; Zhang, W.; Zhang, Z.; Rong, Y.; Zhang, M.; Yu, L.; Zhong, S.; Zhao, R.; Wu, X.; Wong, J. C.; Tang, G. Design and synthesis of orally bioavailable aminopyrrolidinone histone deacetylase 6 inhibitors. *J. Med. Chem.* **2015**, *58*, 2809−2820.
(37) Lee, S.; Lim, D.; Lee, E.; Lee, N.; Lee, H. G.; Cechetto, J.; Liuzzi, M.; Freitas-Junior, L. H.; Song, J. S.; Bae, M. A.; Oh, S.; Ayong, L.; Park, S. B. Discovery of carbohybrid-based 2-aminopyrimidine analogues as a new class of rapid-acting antimalarial agents using image-based cytological profiling assay. *J. Med. Chem.* **2014**, *57*, 7425−7434.
(38) Zheng, Y.; Benet, L. Z.; Okochi, H.; Chen, X. pH Dependent but not P-gp dependent bidirectional transport study of s-propranolol: The importance of passive diffusion. *Pharm. Res.* [Online early access]. DOI: 10.1007/s11095-015-1640-3. Published Online: February 19, **2015**.
(39) Duan, H.; Ning, M.; Zou, Q.; Ye, Y.; Feng, Y.; Zhang, L.; Leng, Y.; Shen, J. Discovery of intestinal targeted TGR5 agonists for the treatment of type 2 diabetes. *J. Med. Chem.* **2015**, *58*, 3315−3328.
(40) Cinelli, M. A.; Li, H.; Chreifi, G.; Martásek, P.; Roman, L. J.; Poulos, T. L.; Silverman, R. B. Simplified 2-aminoquinoline-based scaffold for potent and selective neuronal nitric oxide synthase inhibition. *J. Med. Chem.* **2014**, *57*, 1513−1530.
(41) Plowright, A. T.; Nilsson, K.; Antonsson, M.; Amin, K.; Broddefalk, J.; Jensen, J.; Lehmann, A.; Jin, S.; St-Onge, S.; Tomaszewski, M. J.; Tremblay, M.; Walpole, C.; Wei, Z.; Yang, H.; Ulander, J. Discovery of agonists of cannabinoid receptor 1 with restricted central nervous system penetration aimed for treatment of gastroesophageal reflux disease. *J. Med. Chem.* **2013**, *56*, 220−240.
(42) Over, B.; McCarren, P.; Artursson, P.; Foley, M.; Giordanetto, F.; Grönberg, G.; Hilgendorf, C.; Lee, M. D.; Matsson, P.; Muncipinto, G.; Pellisson, M.; Perry, M. W., 4th; Svensson, R.; Duvall, J. R.; Kihlberg, J. Impact of stereospecific intramolecular hydrogen bonding on cell permeability and physicochemical properties. *J. Med. Chem.* **2014**, *57*, 2746−2754.
(43) Kutchinsky, J.; Friis, S.; Asmild, M.; Taboryski, R.; Pedersen, S.; Vestergaard, R. K.; Jacobsen, R. B.; Krzywkowski, K.; Schrøder, R. L.; Ljungstrøm, T.; Hélix, N.; Sørensen, C. B.; Bech, M.; Willumsen, N. J. Characterization of potassium channel modulators with QPatch automated patch-clamp technology: system characteristics and performance. *Assay Drug Dev. Technol.* **2003**, *1*, 685−693.
(44) Zhou, P. Z.; Babcock, J.; Liu, L. Q.; Li, M.; Gao, Z. B. Activation of human ether-a-go-go related gene (hERG) potassium channels by small molecules. *Acta Pharmacol. Sin.* **2011**, *32*, 781−788.
(45) Lucas, M. C.; Bhagirath, N.; Chiao, E.; Goldstein, D. M.; Hermann, J. C.; Hsu, P. Y.; Kirchner, S.; Kennedy-Smith, J. J.; Kuglstatter, A.; Lukacs, C.; Menke, J.; Niu, L.; Padilla, F.; Peng, Y.; Polonchuk, L.; Railkar, A.; Slade, M.; Soth, M.; Xu, D.; Yadava, P.; Yee, C.; Zhou, M.; Liao, C. Using ovality to predict nonmutagenic, orally efficacious pyridazine amides as cell specific spleen tyrosine kinase inhibitors. *J. Med. Chem.* **2014**, *57*, 2683−2691.
(46) Brodney, M. A.; Beck, E. M.; Butler, C. R.; Barreiro, G.; Johnson, E. F.; Riddell, D.; Parris, K.; Nolan, C. E.; Fan, Y.; Atchison, K.; Gonzales, C.; Robshaw, A. E.; Doran, S. D.; Bundesmann, M. W.;

DOI: 10.1021/jm5020023
J. Med. Chem. XXXX, XXX, XXX−XXX

Buzon, L.; Dutra, J.; Henegar, K.; LaChapelle, E.; Hou, X.; Rogers, B. N.; Pandit, J.; Lira, R.; Martinez-Alsina, L.; Mikochik, P.; Murray, J. C.; Ogilvie, K.; Price, L.; Sakya, S. M.; Yu, A.; Zhang, Y.; O'Neill, B. T. Utilizing structures of CYP2D6 and BACE1 complexes to reduce risk of drug-drug interactions with a novel series of centrally efficacious BACE1 inhibitors. *J. Med. Chem.* **2015**, *58*, 3223−3252.

(47) Díaz, J. L.; Christmann, U.; Fernández, A.; Torrens, A.; Port, A.; Pascual, R.; Álvarez, I.; Burgueño, J.; Monroy, X.; Montero, A.; Balada, A.; Vela, J. M.; Almansa, C. Synthesis and structure-activity relationship study of a new series of selective $\sigma(1)$ receptor ligands for the treatment of pain: 4-aminotriazoles. *J. Med. Chem.* **2015**, *58*, 2441−2451.

(48) Cho, Y. S.; Whitehead, L.; Li, J.; Chen, C. H.; Jiang, L.; Vögtle, M.; Francotte, E.; Richert, P.; Wagner, T.; Traebert, M.; Lu, Q.; Cao, X.; Dumotier, B.; Fejzo, J.; Rajan, S.; Wang, P.; Yan-Neale, Y.; Shao, W.; Atadja, P.; Shultz, M. Conformational refinement of hydroxamate-based histone deacetylase inhibitors and exploration of 3-piperidin-3-ylindole analogues of dacinostat (LAQ824). *J. Med. Chem.* **2010**, *53*, 2952−2963.

(49) Li, T.; Li, N.; Guo, Q.; Ji, H.; Zhao, D.; Xie, S.; Li, X.; Qiu, Z.; Han, D.; Chen, X.; You, Q. Inhibitory effects of wogonin on catalytic activity of cytochrome P450 enzyme in human liver microsomes. *Eur. J. Drug Metab. Pharmacokinet.* **2011**, *36*, 249−256.

(50) Yang, S.; Qiu, Z.; Zhang, Q.; Chen, J.; Chen, X. Inhibitory effects of calf thymus DNA on metabolism activity of CYP450 enzyme in human liver microsomes. *Drug Metab. Pharmacokinet.* **2014**, *29*, 475−481.

(51) Spicer, T. P.; Jiang, J.; Taylor, A. B.; Choi, J. Y.; Hart, P. J.; Roush, W. R.; Fields, G. B.; Hodder, P. S.; Minond, D. Characterization of selective exosite-binding inhibitors of matrix metalloproteinase 13 that prevent articular cartilage degradation in vitro. *J. Med. Chem.* **2014**, *57*, 9598−9611.

(52) Ling, C.; Fu, L.; Gao, S.; Chu, W.; Wang, H.; Huang, Y.; Chen, X.; Yang, Y. Design, synthesis, and structure-activity relationship studies of novel thioether pleuromutilin derivatives as potent antibacterial agents. *J. Med. Chem.* **2014**, *57*, 4772−4795.

DOI: 10.1021/jm5020023
J. Med. Chem. XXXX, XXX, XXX−XXX